CHARACTERIZATION OF A *VIBRIO FISCHERI* MUTANT LACKING THE BROAD-SPECTRUM RACEMASE, BSRV

by

KATHRIN A. LARAMORE

(Under the Direction of Eric V. Stabb)

ABSTRACT

D-amino acids are ubiquitous in nature and their function in microorganisms is an ongoing area of interest. In bacteria, D-Glu and D-Ala are associated with peptidoglycan cell wall, while other non-canonical D-amino acids (NCDAAs) are implicated in a variety of processes. *Vibrio cholerae*'s broad-spectrum racemase, BsrV, produces NCDAAs that affect peptidoglycan structure and strength in stationary phase. Orthologs of BsrV are found in several members of the *Vibrionaceae*, and I investigated the role of BsrV in *Vibrio fischeri.* A *V. fischeri bsrV* mutant had reduced D-amino acid production, attenuated growth in low-salt media, and subtly altered peptidoglycan structure. The *bsrV* mutant was unaffected in its symbiosis with *Euprymna scolopes* but out-competed the wild type when cultured in a high-salt medium, revealing a fitness cost to harboring *bsrV*. This study illustrates distinct functions for BsrV between similar organisms and provides a foundation for additional research on BsrV-produced D-amino acids.

INDEX WORDS: D-Amino Acids, BsrV, peptidoglycan, *Vibrio fischeri*, *Euprymna scolopes*,

CHARACTERIZATION OF A *VIBRIO FISCHERI* MUTANT LACKING THE BROAD-SPECTRUM RACEMASE BSRV

by

KATHRIN A. LARAMORE

B.S. Microbiology, California Polytechnic State University of San Luis Obispo, 2017

A Thesis Submitted to the Graduate Faculty of The University of Georgia in Partial Fulfillment of the Requirements for the Degree

MASTER OF SCIENCE

ATHENS, GEORGIA

2020

CHARACTERIZATION OF A *VIBRIO FISCHERI* MUTANT LACKING THE BROAD-SPECTRUM RACEMASE, BSRV

by

KATHRIN A. LARAMORE

Major Professor:	Eric V. Stabb
Committee:	Vincent Starai
	Ellen Neidle

Electronic Version Approved:

Ron Walcott
Interim Dean of the Graduate School
The University of Georgia
May 2020

DEDICATION

This thesis is dedicated to my family. My parents, my grandma, my brother, my nephew, and my Nick. Your positivity, support, and belief in my abilities has enabled my success and reminded me that I am a whole and accomplished person. I am lucky to be loved by you.

ACKNOWLEDGEMENTS

I would like to first and foremost acknowledge my mentor, Eric, whose professional and scientific guidance has been invaluable. I would like to thank him for allowing me the freedom to ask any question and feel confident in my abilities. I would like to acknowledge my committee members, Ellen Neidle and Vinny Starai. I will always be grateful for their support and guidance during an uneasy transition. I would like to acknowledge and thank Janice Stuart for her patience with my endless questions and ideas for the department. I would like to acknowledge the Microbiology Graduate Advisory Committee, and in particular Jessica Irons and Abigail Calixto. These women are inspiring badasses who pushed me to think critically about ideas beyond the bench. I would like to thank and acknowledge past and present Stabb Lab members. In particular, special thanks to Kathryn Bellissimo, Coralis Rodriguez-Garcia, and Macey Coppinger for making an uneasy time more fun and lighthearted. Last but not least, I would like to thank my partner Nick Stair, whose patience, love, support, and conversations allow me to dream big about all of the adventures waiting for us beyond Georgia.

TABLE OF CONTENTS

LIST OF TABLES

Page

LIST OF FIGURES

Page

CHAPTER 1

INTRODUCTION AND LITERATURE REVIEW

OVERVIEW

Amino Acids, both D- and L- enantiomer forms, are ubiquitous in nature and essential in biological systems. L- amino acids are the building blocks for proteins and therefore serve as a foundation for life on earth. D-amino acids also serve a fundamental role in biology: D-Glu and D-Ala are incorporated into peptidoglycan (PG), the mesh-like polymer that provides strength to bacterial cell walls (1). PG is a dynamic structure that is continuously remodeling during growth and development. Its relatively conserved structure makes it an ideal target for antibiotics and for the bacteria-surveillance systems in plants and animals. It is therefore important to understand the regulation of, and structural deviations in, PG composition (2). Non-canonical D-amino acids (NCDAAs), or those that are not constituents of archetypal PG, can be found in PG, where they modulate its function, and have roles in other microbial process. Such processes for NCDAAs include using them as carbon and nitrogen sources (3, 4), and producing them to aid in competitive inhibition (5), biofilm dispersal (6-11), and growth-phase transitions (12-14). Interestingly, the antimicrobial properties of D-Arg, which is produced by some bacteria, can be overcome by mutations in a conserved phosphate-transport system, suggesting a role for D-Arg either in the regulation of phosphate uptake or in microbial competition for this resource (5).

BsrV, a broad-spectrum racemase originally identified in *V. cholerae,* is hypothesized to be the primary producer of microbial NCDAAs in many members of the Vibrionaceae (13, 15). I have focused on the BsrV ortholog in the model organism *Vibrio fischeri*, a species that participates in a bacterial-animal mutualism within the light organ of the Hawaiian bobtail squid, *Euprymna*

scolopes. Advantages of this model include its safety as a non-pathogen, its parallels to important pathogens such as *V. cholerae*, and its ability to colonize *E. scolopes* as a monoculture, enabling controlled experiments under natural (i.e., symbiotic) conditions (16).

D-AMINO ACIDS

Every amino acid, excluding glycine, occurs in two different stereoisomers, D- and L-, around the α-carbon. All known living organisms use L-amino acids as the building blocks for proteins. The uses of less common D-isomers are more mysterious, but they do have known biological roles. Some are found in microbial cell walls as key constituents of the PG peptide chain, while others are produced for yet unknown functions (2, 12). D-amino acid production typically occurs through the racemization of an L-enantiomer counterpart. Two types of racemases have been described: Pyridoxyl-5-Phosphate (PLP)-dependent and PLP-independent racemases. PLP-dependent racemases include the highly specific racemases of alanine, serine, and lysine (17). Of these highly specific racemases, alanine racemases have been described in almost all peptidoglycan-producing bacteria (17). Also falling into the category of PLP-dependent racemases is the newly described family of broad-spectrum racemases (Bsr) contained primarily within the phylum *Proteobacteria* (18). In contrast to the highly specific amino acid racemases, the Bsr's can use up to nineteen natural chiral amino acids as substrates (15). The PLP-independent racemases that have been described include aspartic acid, proline, and glutamic acid racemases, the latter being the most abundant within this group due to D-Glu's role in PG (19-21).

D-amino acids are found ubiquitously in nature and can originate from a variety of sources other than bacterial cell walls. They are prevalent in soil and are derived from antibiotics, synthetic insecticides, feces, plants, and animals, in addition to microbes (22). Moreover, L-amino acids in

the environment are subject to both the biotic and abiotic racemization to their D-enantiomers. Abiotic racemization is influenced by factors such as pH, heat, presence of aldehydes, salts, and radiation, while racemases are the biotic catalysts of racemization (23). Free D-amino acids in the marine environment may be of particular interest as many D-amino acids, such as D-Ala and D-Asp, are both released and catabolized by marine Bacteria and Archaea (24).

In the sections below I will briefly summarize what is known about D-amino acids in the biosphere, and I will focus on a relatively recently discovered class of broad-spectrum racemases capable of interconverting a number of D-amino acids. I will then describe the model symbiosis between *V. fischeri* and *E. scolopes*, which I used to explore potential roles for one such broad-spectrum racemase.

ROLES OF D-AMINO ACIDS IN BIOLOGICAL SYSTEMS

D-amino acids in peptidoglycan (PG)

PG is a robust and dynamic polymer that comprises the main constituent of most bacterial cell walls. PG is responsible for maintaining cell shape and size, supporting osmotolerance in changing environments, and it serves to anchor cell envelope components such as proteins and lipoteichoic acids (25-27). PG must be strong enough to withstand environmental pressures yet elastic enough to adapt to cellular growth and division (2).

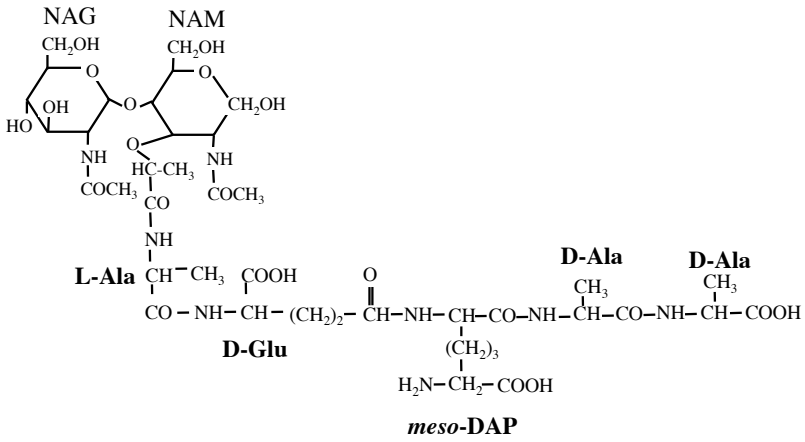

Figure 1.1. Peptidoglycan structure. Shown is the ß-(1,4) linked NAG and NAM dissaccharide bound to the pentapeptide (residue identities in bold text) common to most Gram-negative organisms inlcuding *V. fischeri*.

The PG polymer in most bacteria is made up of alternating residues of ß-(1,4) linked *N*-acetylglucosamine (NAG) and *N*-acetylmuramic acid (NAM). NAM residues are connected to a pentapeptide chain (Figure 1.1). In *V. fischeri* and most Gram-negative bacteria, the pentapeptide chain consists of L-alanyl-D-γ-glutamyl-*meso*-diaminopimelyl-D-alanyl-D-alanine (L-Ala- γ-D-Glu-mDAP-D-Ala-D-Ala). PG monomers are cross linked together through mDAP residues or mDAP and D-Ala residues and the terminal D-Ala residue is lost in the mature macromolecule (2, 28). Although this structure is well conserved among Prokaryotes, variations in the PG peptide chain have been observed (Table 1.1). For example, D-Ala in the 4th position has been substituted for Glycine and D-serine in *Microbispora* and D-Met in *Vibrio cholerae* (2). The presence of D-amino acids in bacterial cell walls protect the peptidoglycan from proteases, which have evolved to cleave between L-amino acids (23). It is possible that the presence of some D-amino acids may impact the organism's resistance to radiation and/or extreme heat, such as the L-Orn-containing PG in *Deinococcus radiodurans* or *Thermus thermophilis* (2, 29, 30).

Table 1.1. Modifications to peptidoglycan pentapeptide[a]

Position	Amino acid (in *V. fischeri*)	Substitutions	Examples
1	L-Ala	Gly	*Mycobacterium leprae*
		L-Ser	*Butyribacterium rettgeri*
2	D-Glu	D-Gln	Many G+[b], *Mycobacteria*
		3-OH-Glu	*Microbacterium lacticum*
3	*meso*-DAP	L-Lys	Most G+
		Lanthionine	*Fusobacterium nucleatum*
		L-Orn	Spirochetes, *Dinococcus radiodurans, Thermus thermophilis*
		L-homoserine	*Corynebacterium poinsettiae*
4	D-Ala	Gly	*Microbispora*
		D-Ser	
		D-Met	*Vibrio cholerae, E. coli* (13, 31)
5	D-Ala	D-Ser	*Enterococcus gallinarum*
		D-Lac[c]	*Lactobacillus casei,* Vancomycin-resistant *Enterococci*

[a] Modified from Vollmer *et al* (2) with modifications based on (13, 31).
[b] G+ indicates Gram-positive bacteria
[c] D-Lactate is found in the 5th position of PG monomers in strains with natural or acquired resistance to vancomycin (32).

D-amino acids as growth substrates

Given their use in proteins, it is not surprising that L-amino acids are often readily used as growth substrates; however, some microorganisms have evolved the ability to utilize both L- and D-amino acids as nutrient sources. Although typically less abundant than their L- counterparts, D-amino acids can nonetheless provide important resources, especially when other nutrients are scarce or when competition favors niche diversification and/or resource-use diversification. In the environment, microbes may encounter D-amino acids as nutrients in deep-sea and aquatic

environments, within plant and animal tissues, and from microbially sourced PG fragments (24, 33-36). Although the biological fates of environmental D-amino acids are not fully understood, there are known examples of D-amino acid use by specific bacteria.

One example is *Pseudomonas aeruginosa,* which is able to metabolize many D-amino acids. D-Ala, D-His, D-Phe, D-Ser, D-Thr, and D-Val are catabolized by a D-amino acid dehydrogenase (DadA) with broad substrate specificity and the amino acid racemase DadX, both of which are encoded by the *dadAX* operon (3). *P. aeruginosa* also catabolizes D-Glu and D-Gln via the proteins encoded by the *dguRABC* locus (3, 4). Other microorganisms including *Escherichia coli, Helicobacter pylori, Proteus mirabilis, Sinorhizobium meliloti, Candida boidinii,* and recently isolated organisms from deep-sea sediments also have been shown to hold similar catabolic pathways for D-amino acids (34, 37-43).

In at least two cases, bacteria use LysR-type transcriptional regulators (LTTR) to efficiently respond to the presence of D-amino acids and induce catabolic pathways. One such LTTR, DguR, is encoded within the *dguRABC* operon of *P. aeruginosa* PAO1 and directs the catabolism of D-Glu when this amino acid is present (4). As D-Glu is a constituent of microbial PG, it is possible that this pathway serves as a mechanism for scavenging environmental PG. *V. fischeri*, the model organism that is the focus of this thesis, possesses a D-Asp-responsive LTTR, DarR, which is responsible for the transcriptional induction of an Asp racemase (44), thereby allowing D-Asp to be used as a carbon and/or nitrogen source. The specificity of these transcriptional regulators for certain D-amino acids suggests that D-amino acids are the natural targets for their respective catabolic loci.

D-amino acid-containing products of nonribosomal peptide synthetases (NRPSs)

Investigation of bioactive natural products has been a topic of considerable interest since 1929, when Alexander Fleming uncovered the antibacterial activity of penicillin, a peptide derivative produced by *Penicillium notatum* (45). Many of these bioactive products and peptides contain D-amino acids and are generated by large enzymes called nonribosomal peptide synthetases (NRPSs) (46). To produce these D-amino acid-containing peptides, NRPSs activate and convert L-amino acid substrates to the D-forms before coupling it to the peptidyl intermediate (47). NRPS products that contain a D-amino acid moiety are endowed with unique activities compared to peptides comprising only L-amino acids (47). For example, the D-amino acid-containing dipeptide cyclo(D-Tyr-D-Phe) accumulates in the supernatant of *Bacillus* sp. strain N, isolated from certain entomopathogenic nematodes. This dipeptide inhibits the growth of *Staphyloccocus epidermidis* and *Proteus mirabilis* significantly more than the dipeptides containing only the L-forms (47, 48). It is hypothesized that the incorporation of D-amino acids into NRPS products increases stability against proteolytic digest and favors unique conformations important for biological activity (46).

D-amino acids in Eukaryotes

D-Asp and D-Ser are suggested to be the only two D-amino acids originating directly from racemization of L-amino acids within human tissues, and considerable research has focused on the role of these D-amino acids in human physiology (49). It is now well established that these D-amino acids contribute to multiple processes in the human central nervous system. For example, serine racemases are expressed in neurons in the forebrain and hippocampus (50, 51). The fundamental role of D-Ser in the brain is as a co-agonist/binding substrate at the *N*-methyl-

D-Aspartate Receptor (NMDAR) that is involved in synaptic plasticity, which controls neuronal communication (52, 53). Abnormal D-Ser levels in the brain have been linked to neurological health problems related to aging, Alzheimer's disease, and amyotrophic lateral sclerosis (54-56). D-Asp also plays fundamental roles in neurotransmission in addition to having roles in the neuroendocrine system in both humans and rodents (19, 57). Notably, D-Asp is implicated in the development and neurogenesis of the brain, while also being involved in multiple endocrine processes, such as synthesis of hormones in the pituitary gland and the regulation of testosterone release (57, 58).

D-amino acids as interkingdom signaling molecules

Recent research suggests that D-amino acids could act as signaling molecules between Eukaryotes and Bacteria, in both mutualistic and pathogenic contexts. An example of this interkingdom signaling can be found inside the mammalian intestinal tract, where prokaryotes are both diverse and abundant (59). In one study, specific pathogen-free (but not germ-free) mice contained large quantities (200 to 500 nanomole per gram intestinal tissue) of free D-amino acids derived from their gut microbiota. The microbially-derived D-amino acid pool induced the production of D-amino acid oxidase (DAO) by intestinal epithelium cells (40). This microbiota-regulated enzyme catalyzes the oxidative deamination of D-amino acids to produce H_2O_2, an antimicrobial product as part of a host innate immune response (60). This example illustrates how microbiota-derived D-amino acids act as important regulators of bacterial-animal homeostasis. Additionally, accumulating evidence suggests that the production of H_2O_2 by DAO leads to apoptosis of tumor cells, and this mechanism has recently been implicated as a potential cancer treatment and detection strategy. Theoretically, this DAO-mediated process can be regulated by

the administration of D-amino acids, such as D-Ala, which are not endogenously present in human tissues at high levels (19, 61).

Eukaryote-derived D-amino acids can also act to regulate colonization of pathogenic prokaryotes within the host tissues (62). Host-derived D-Serine, which is antimicrobial, selectively suppresses the expression of the *Escherichia coli* O157:H7 (enterohaemorrhagic intestinal *E. coli*) Type-III secretion system, thereby preventing the injection of effectors that facilitate *E. coli's* attachment to host cells and efficient colonization (63, 64). Thus, just as host cells recognize and respond to microbially produced D-amino acids, so too do bacteria detect and respond to host-generated D-amino acids. This two-way detection of D-amino acids in symbiotic systems could represent a subtle but important aspect of these associations and merits further investigation.

Microbial community regulation by D-amino acids

D-amino acids can act not only as interkingdom cues, but also as signals within bacterial communities. The effects of microbially produced D-amino acids on various behaviors in diverse bacterial species have been explored, albeit with mixed results. For example, D-Tyr inhibits growth and indirectly decreases biofilm formation in both *Bacillus subtilis* and *Pseudomonas aeruginosa* at low, sublethal concentrations. However, when the mechanism of biofilm inhibition was investigated further, opposing effects of D-amino acids were observed with respect to exopolysaccharide (EPS) production. In *B. subtilis,* EPS increased with respect to the biofilm while it decreased in *P. aeruginosa* (7). In a particularly broad study, the activity of eighteen different D-amino acids toward *Acinetobacter baumannii* and *P. aeruginosa* was evaluated. In *A. baumannii,* D-Cys, D-Trp and D-His decreased biofilm formation, reduced attachment to A549 human alveolar epithelial cells, and inhibited growth. In contrast, D-amino acids seemed to have

no toxic effects on *P. aeruginosa*, and D-alanine and D-glycine instead induced biofilm production and enhanced growth by acting as a nutrient source (8). D-amino acids appear to exhibit differential effects on bacterial biofilm formation, with the outcome being highly dependent on the experimental setup (6, 8-11).

There is some evidence to suggest that D-Arg production by a broad-spectrum racemase, BsrV, in *V. cholerae* can control growth dynamics of neighboring microorganisms in synthetic bacterial communities. The growth of *Caulobacter crescentus,* a particularly D-Arg sensitive microbe, was inhibited by the BsrV-dependent production of D-Arg, while a *V. cholerae* strain that was unable to produce D-Arg had no effect on the community growth dynamics. The community control via D-amino acids hypothetically offers a fitness advantage to both the generator of the effectors and to organisms that are resistant to D-amino acids (5).

BsrV-produced NCDAAs can also trigger changes in PG structure. When grown in exogenous D-Met, which is also produced by BsrV, many organisms (e.g., *V. cholerae, C. crescentus, Enterococcus faecalis,* and *B. subtilis*) can incorporate this D-amino acid into the 4th position of the peptide side chain, replacing D-Ala in a fraction of the stationary phase PG (13, 14, 31). If many bacterial species are able to incorporate NCDAAs into their muropeptides whether or not they produce them, it is possible that D-amino acid production by BsrV-containing organisms could influence the PG structure of nearby cells in microbial communities. BsrV is implicated as the originator of D-Met as well as many other NCDAAs, and these PG alterations are hypothesized to provide fitness in stationary phase conditions (12, 13). Combined, this research highlights how D-amino acids exhibit differential roles in bacterial species and confer varying fitness advantages depending on the organism.

D-amino acids' role in regulating growth phase transitions in bacteria

Microbes are seldom presented with ideal conditions for supporting continuous growth. During stationary phase, microbes are forced to adapt quickly to changing situations and compete in nutrient scarcity (65). D-amino acids are one type of cue to regulate the growth phase transitions of the bacterial cells that produce them. For example, D-amino acids appear to regulate spore germination. Bacterial sporulation is the highly regulated process where cells become metabolically latent and resistant to conditions that are harsh or lacking nutrients (66). D-Ala was found to inhibit spore germination in many *Bacillus* species, and later investigation revealed that *Bacillus* species use D-Ala as an auto-inhibitor at high spore density when L-Ala (a spore germinant) is converted to D-Ala (an anti-germinant) by an alanine racemase (67, 68).

PG structure is continuously remodeled to change cell size during growth and division, to accommodate structures that span the PG, to provide the appropriate strength and flexibility in changing environments, and to control cell shape. Wild-type *V. cholerae* typically displays a curved-rod cell morphology, although the degree of curvature is dependent on cell density and environmental factors (69). Investigation of this cell curvature led to the discovery of a role for NCDAAs and BsrV. Specifically, a *mrcA* mutant found in a screen for cell-shape defects showed no difference from the parent in exponential phase but had coccoidal cell morphology upon the transition to stationary phase. The *mrcA* gene encodes the inner-membrane-anchored enzyme PBP1A that is involved in the synthesis of cross-linked PG (2, 70). Surprisingly, the rod-to-sphere transition of Δ*mrcA* cells could be triggered at any growth phase by the addition of extracellular NCDAAs, D-Met, D-Leu, D-Val, and D-Ile, which were present in the stationary phase supernatants. The aforementioned broad-spectrum racemase BsrV was shown to generate these NCDAAs (13).

V. cholerae strains lacking *bsrV,* and therefore lacking the ability to produce NCDAAs, had twice the amount of PG within their cell walls during stationary phase, reduced length in PG glycan chains (~80% relative to wild-type), and were twenty fold more sensitive to lysis during osmotic challenge (13). Growth of the *bsrV* mutant in exogenous D-Met and D-Leu returned PG quantity and length of glycan chains to wild-type levels, indicating that these BsrV-dependent NCDAAs are responsible for the PG alterations observed in stationary phase *bsrV* mutants. D-Met was also incorporated into the PG itself. Thus, these D-Amino acids initiated stationary phase PG remodeling in wild-type cells and thereby controlled the quantity and strength of PG. The expression of BsrV in *V. cholerae* is triggered by the alternative sigma factor RpoS, which becomes activated upon entry to stationary phase (14, 71). All aforementioned phenotypes associated with BsrV thus far are dependent on stationary phase growth, suggesting its role in stationary phase transitions and adaptations to the stresses of environmental changes during stationary phase.

Broad-spectrum racemase, BsrV

As described above, the broad-spectrum racemase BsrV from V. *cholereae* has generated considerable interest. While some racemases like MurI and Alr have a high degree of substrate specificity for interconverting D- and L-forms of glutamate and alanine, respectively, Bsr's are able to produce D-amino acids from both proteinogenic and non-proteinogenic L-amino acids (15, 72). Bsr's are found in many bacterial species associated with various environments (water, soil, host-associated). Interestingly, of the seventy-four racemases bioinformatically grouped into the Bsr family, all known are found within the phylum *Proteobacteria* and most are found in marine organisms, with just over half belonging in the *Vibrionaceae* family (15).

Racemases with similar enzymatic properties have been reported in *V. cholerae, Proteus mirabilis, Oenococcus oeni, Pseudomonas taetrolens, and Pseudomonas putida* (13, 15, 73-76). The seminal and most extensive preceding work on Bsr's have been done in the *V. cholerae* model on the archetype, BsrV. BsrV is similar to Alr, the primary and substrate-specific alanine racemase required for PG biosynthesis in many bacteria (15). BsrV is a PLP-dependent racemase that forms a dimer and can act on nineteen different natural chiral amino acids *in vitro.* Notably, Alr's are cytoplasmic proteins while all BsrV orthologs contain signal peptides to direct them to the periplasm (15).

The preceding work on BsrV and NCDAA production has been almost entirely explored within pathogenic *V. cholerae*. The study of BsrV in *Vibrio fischeri,* a BSL-1 organism, offers two main advantages. First, *V. fischeri* participates in a model bacterial-animal symbiosis. If BsrV or its NCDAA production plays an important role during colonization of animal hosts by Vibrios, the *V. fischeri-E. scolopes* mutualism (described below) is an ideal, tractable, and natural model to explore how and why this might be the case. Second, if BsrV plays a role outside of the mutualism, it is safer and easier to work with a BSL-1 non-pathogen.

MODEL *VIBRIO-EUPRYMNA* SYMBIOSIS

Many *Vibrio* species have been isolated from animal hosts, either as enteric commensals or as pathogens, but the monospecific light-organ symbiosis between *V. fischeri*, a bioluminescent marine microbe, and the Hawaiian Bobtail Squid, *Euprymna scolopes* provides a uniquely tractable experimental model for bacterial-animal associations (16, 77, 78). The *V. fischeri* wild-type strain that is most commonly used in the laboratory is ES114, which was isolated from wild squid (79, 80). It is easily cultured; its genome has been sequenced, it is genetically tractable, and

it readily infects the light organ of *E. scolopes* hatched in captivity (81-83). The squid readily breed and lay eggs in the laboratory (16, 84). Given these reasons and many others, this model microbe-animal association proves amenable to laboratory investigation with a great deal of experimental control. Prior research into the *Vibrio-Euprymna* mutualism has provided insights into the evolutionary underpinnings and physiological mechanisms of persistent, symbiotic relationships (85-87). Therefore, it should likewise be a good model for testing whether BsrV's and NCDAAs play an important role in *Vibrio*-host interactions.

V. fischeri exists as both as a free-living and host-associated marine microbe. *V. fischeri* monospecifically infects the ventrally located light organ of *E. scolopes* (78, 88). The juvenile squid are aposymbiotic when they emerge from the egg, and infection by environmental *V. fischeri* cells occurs within hours of hatching (89). In the light organ of the squid, the symbiont provides its host with bioluminescence in exchange for a growth-promoting environment (90). The bioluminescence is thought to aid the host by providing counterillumination that *E. scolopes* individuals use to camouflage themselves; by matching the intensity of bacterial bioluminescence emitted from their light organ with the down-welling moonlight and starlight, they can reduce the appearance of their silhouette to predators or prey beneath them in the water column (90).

The *E. scolopes* light organ contains three sacculate crypts, each with a pore on the surface connected to a ciliated duct (Figure 1.2). Infection of the light organ is initiated when the *V. fischeri* cells present in the seawater are propelled by ciliated epithelial appendages (CEAs) to accumulate and congregate in a host-derived field of mucus near the pores (91). Here, *V. fischeri* cells aggregate and are enriched relative to other Gram-negative bacteria that also adhered to the mucus (92). After 2-3 h of congregation, *V. fischeri* cells, propelled by flagella, swim through the pores, migrate up the ducts, and colonize the antechambers and crypts (88). The *V. fischeri* cells grow in

the crypts and establish a persistent symbiosis with an initial doubling time of approximately 20 min (89, 93, 94). The colonization by *V. fischeri* triggers the regression and disappearance of the CEAs, and the monospecific culture of *V. fischeri* persists for the remainder of the squid's life (86, 95-97). The squid are nocturnally active and are found buried under the sand during daylight hours (80, 98). At dawn, light cues the *E. scolopes* to vent 90% of the *V. fischeri* cells into the environment, and the remaining microbes re-grow a fresh culture to support counterillumination in the evening (80, 86, 90, 98, 99).

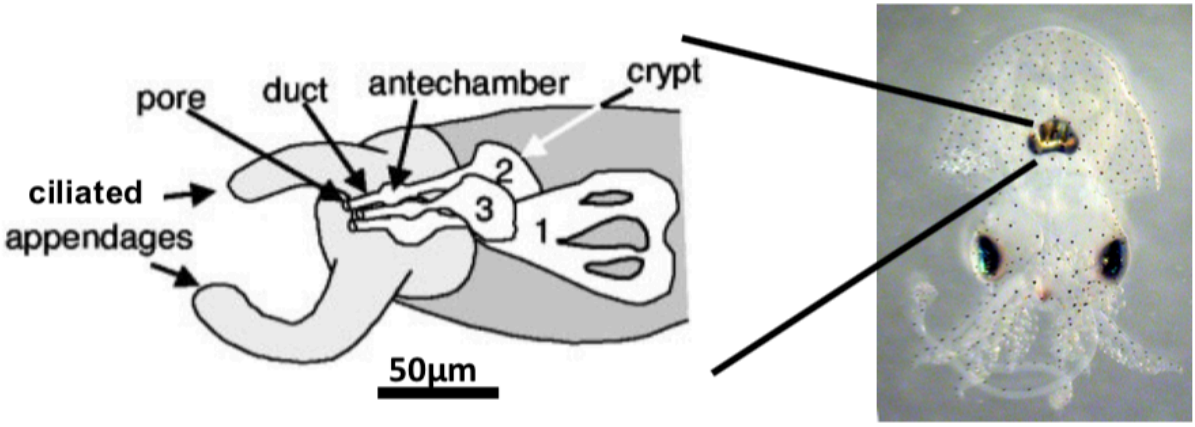

Figure 1.2. Diagram of the juvenile squid light organ. (Right) Juvenile squid. (Left) Schematic representation of one lobe (one half) of a juvenile *E. scolopes* squid light organ. Three pores are located at the base of the ciliated epithelial appendages (CEAs). These pores lead through ducts, to antechambers, and eventually crypt spaces (numbered 1-3). The crypts house most of the *V. fischeri* culture. Figure courtesy of Eric Stabb.

SUMMARY

D-amino acids are widespread in the environment and produced by many biological systems, including microorganisms. In addition to their potential uses as nutrient sources, several roles have been proposed for D-amino acids in bacteria, including potential functions as structural or signaling molecules. The periplasmic broad-spectrum racemase, BsrV, of *V. cholerae* has been the subject of particular interest, given its ability to produce NCDAAs that are incorporated into

PG and/or inhibitory toward other microbes. In the remainder of this thesis, I will describe my studies of BsrV in *V. fischeri*. My goals were to compare and contrast the function of BsrV's from *V. fischeri* and *V. cholerae*, to test whether BsrV plays a role in *V. fischeri*'s symbiosis with *E. scolopes*, and to lay the foundation for using *V. fischeri* as a model for studying BsrV.

CHAPTER 2

CHARACTERIZATION OF BSRV IN *VIBRIO FISCHERI*[1]

[1]Laramore, K.A., Stabb, E.V. To be submitted to *Journal of Bacteriology*.

ABSTRACT

D-amino acids are ubiquitous in nature, and there is growing interest in microbial sources and uses for these enantiomers of their proteinogenic L-amino acid counterparts. In bacteria, D-Glu and D-Ala are associated with the archetypal structure of peptidoglycan (PG), while other D-amino acids, termed non-canonical D-amino acids (NCDAAs) have been implicated in competitive inhibition, nutrient scavenging, and cell wall remodeling. For example, *Vibrio cholerae*'s broad-spectrum racemase, BsrV, produces NCDAAs in stationary phase that affect cell-wall structure and increase resistance to low-salt osmotic stress. Orthologs of BsrV are found in several members of the *Vibrionaceae* family, and we investigated the roles of BsrV in the bacterium *Vibrio fischeri.* We found that wild-type *V. fischeri* releases D-amino acids into the medium during growth, whereas a *bsrV* mutant did not. Consistent with BsrV's contribution to PG structure and osmotolerance in *V. cholerae*, the *V. fischeri bsrV* mutant had subtle alterations in its PG, and its growth was inhibited relative to the wild type in low-salt media. Interestingly, the *bsrV* mutant out-competed wild-type in a high-salt medium, revealing a previously undescribed fitness cost to *bsrV*. Finally, the *bsrV* mutant was unaffected in initiating *V. fischeri*'s symbiosis with the Hawaiian bobtail squid, *Euprymna scolopes.* This study illustrates distinct functions for BsrV between similar organisms and lays a foundation for additional study on the roles of BsrV-produced D-amino acids.

INTRODUCTION

With the exception of glycine, all amino acids have four unique functional groups and can exist as one of two enantiomer forms (L- and D-), which as mirror images can serve different biological purposes. L-amino acids act as the fundamental components of proteins while D-amino

acids, predominantly D-Ala and D-Glu, are key constituents of the peptidoglycan (PG) component of bacterial cell walls (2). PG is a glycan polymer that forms a strong network within the cell wall, thereby reinforcing the cell to withstand environmental changes and stress (2, 70). To serve this function, PG needs to be both elastic and resilient in order to retain proteins anchored to the cell envelope, maintain osmotolerance, and modulate cell size and shape to adapt to cellular growth and division (1, 2, 70).

Though the most well-known D-amino acids are the D-Ala and D-Glu constituents of PG, recent observations indicate that diverse bacterial species produce also other D-amino acids, which are collectively known as Non-canonical D-amino acids (NCDAAs). Bacterially produced NCDAAs can accumulate to low millimolar concentrations in stationary phase cultures (5, 13) and have recently gained attention for their roles in varying processes such as competitive inhibition (5), biofilm formation (6-11), and stationary phase PG remodeling (12-14). Environmental NCDAAs, produced through both biological and abiotic process, also serve as growth-supporting sources of carbon and nitrogen (3, 4).

Biological production of D-amino acids usually is dependent on the racemization of their L-enantiomer counterparts (17, 18). For the most abundant PG-associated D-amino acids, D-Ala and D-Glu, racemization of L-Ala and L-Glu is catalyzed by highly specific, Pyrodoxyl-5-phosphate (PLP)-dependent racemases Alr and MurI, respectively (15, 17, 72). In contrast, the production of NCDAAs often appears to be dependent on a family of broad-spectrum racemases (Bsr) (30). BsrV of *V. cholerae* has been the most studied of the Bsr's, serving as an archetypal NCDAA-producing enzyme. BsrV is a periplasmic, PLP-dependent racemase that catalyzes the reversible racemization of nineteen natural chiral amino acids (30). Early research demonstrated that BsrV produces D-Met and D-Leu, which are incorporated into PG and accumulate in the

supernatants of stationary phase *V. cholerae* cultures (13). This incorporation of unusual D-amino acids appears to affect osmotolerance and quantity of PG during stationary phase (13, 31).

These structural changes to PG have been hypothesized to regulate the strength and quantity of the polymer, which could attenuate stationary phase stresses in culture such as the need for decreased synthesis of PG in the face of nutrient scarcity and adaptations to maintain turgor pressure (2, 13, 65, 100). This line of thought is supported by the fact that expression of BsrV in *V. cholerae* is triggered as cells enter stationary phase, controlled by the stress-associated alternative sigma factor, RpoS (14, 71).

In this study, we investigate BsrV's role in a different model organism, *Vibrio fischeri.* This model offers us two unique opportunities. First, *V. fischeri* allows us to study the roles of NCDAAs in a safe, non-pathogenic, BSL-1 organism. Additionally, *V. fischeri* allows us to study roles NCDAAs may play in the model bacterial-animal symbiosis between *V. fischeri* and its host, the Hawaiian Bobtail Squid (*Euprymna scolopes*). We demonstrate that like the archetypal BsrV in *V. cholerae,* BsrV in *V. fischeri* functions to produce D-amino acids, alter PG structure, and confer osmotolerance to low salinity environments. We establish that BsrV is not essential nor does it offer a competitive advantage when colonizing *E. scolopes* and describe a previously unknown fitness burden of NCDAA-production by BsrV.

MATERIALS AND METHODS

Bacterial strains and culture conditions. The strains used in this study are listed in Table 2.1. *V. fischeri* strain ES114, an isolate from the light organ of *E. scolopes*, was used as the wild type and parent for strain construction (79). *E. coli* strains DH5α or DH5αλ*pir* were used as hosts for plasmids, with the latter used to replicate plasmids with the R6K origin of replication (101,

102). Plasmids were transferred from *E. coli* to *V. fischeri* using a previously described triparental mating method and conjugative helper plasmid CC118λpir (pEVS104) (82).

E. coli was grown in lysogeny broth (LB) at 37°C (103). *V. fischeri* was grown at 28°C in either lysogeny broth salt (LBS) medium (104), seawater tryptone (SWT) medium where seawater was replaced by Instant Ocean (105), or a minimal defined medium which consisted of 10 mM $CaCl_2$, 2 μM $FeSO_4$, 2 mM glyceraldehyde-3-phosphate (G3P), 5 mM ribose, 20 mM *N*-acetylglucosamine, 100 mM Tris buffer (pH 7.5), 400 mM NaCl, 10 mM KCl, and 50 mM $MgSO_4$. Solid media was prepared with the addition of 15 g/L agar. For the selection of plasmids in *E. coli,* kanamycin or chloramphenicol was added to LB at final concentrations of 40 or 20 μg/mL, respectively. To maintain plasmids in *V. fischeri,* chloramphenicol was added to LBS at 2 μg/mL.

DNA and plasmid manipulations. Standard cloning methods were used to generate plasmids, and key constructs are listed in Table 2.1. Restriction enzymes and DNA ligase were obtained from New England Biolabs (Ipswich, MA). Plasmids were isolated using ZymoPURE plasmid miniprep kits (Zymo Research, Tustin, CA). The Zero Blunt TOPO PCR cloning kit was used to clone PCR products into pCR-BluntII-TOPO (Invitrogen). DNA fragments were cleaned using a DNA Clean & Concentrator kit (Zymo Research, Tustin, CA). PCR was performed using Phusion High Fidelity PCR Master Mix with HF Buffer or One*Taq* Hot Start 2X Master Mix (New England Biolabs, Ipswich, MA) following manufacturer's recommendations for cycle programs based on predicted DNA-product size. Oligonucleotides were obtained from Integrated DNA Technologies (Coralville, IA). PCR was performed using a C1000 Touch Thermal Cycler (BioRad, Hercules, CA). Sequencing was conducted at the University of Michigan Advanced Genomics core (Ann Arbor, MI).

Construction of mutants and complementation of plasmids. The ~2-kb region upstream of *bsrV* was PCR amplified using primers RJ14 and RJ28, and the ~1.5-kb region downstream of *bsrV* was PCR amplified using primers RJ29 and RJ30. The upstream and downstream fragments were digested with SalI, ligated, gel purified, and cloned into pCR-BluntII-TOPO (Invitrogen). The resulting plasmid, pRMJ13, was sequenced to confirm the Δ*bsrV* allele. To generate a plasmid that could be mobilized by conjugation, the *oriT*-containing plasmid pEVS118 was fused with pRMJ13 by digesting each plasmid with KpnI and ligating them together. The Δ*bsrV* allele on the resulting plasmid, pRMJ14, was mobilized into ES114, and the *bsrV* mutant KL3 was generated by a two-step process of allelic exchange. First clones were identified with pRMJ14 recombined into the chromosome, and then mutants where the Δ*bsrV* allele had replaced *bsrV* were identified based on screening for the loss of antibiotic resistance conferred by the integrated pRMJ14, which could either result in allelic replacement or reversion to wild type. The second step of allelic replacement of *bsrV* with Δ*bsrV* was performed with exogenous D-Ala added to the LBS medium at 40 μg/mL. Allelic exchange was confirmed in the Δ*bsrV* mutant, KL3, by PCR with primers MNC22 and MNC23.

To generate a complementation vector, *bsrV* was PCR amplified using primers KAL1 and KAL2, and the fragment was cloned into pCR-BluntII-TOPO (Invitrogen). Digestion of the resulting plasmid with NheI removed the *bsrV* fragment, which was ligated into NheI-linearized pVSV105, a low-copy shuttle vector derived from a native *V. fischeri* plasmid. Sequencing confirmed the *bsrV* sequence in the resulting plasmid, pKAL6, which was then mobilized into KL3 (Δ*bsrV*) and ES114 (wild type).

Table 2.1. Bacterial strains, plasmids, and oligonucleotides

Strain or Plasmid	Genotype[a]	Source
Escherichia coli		
DH5α	φ80d*lacZ*ΔM15Δ (*lacZYA-ARGF*)U169 *deoR supE44 hsdR17recA1 endA1 gyrA96 thi-1 relA1*	(102)
DH5α λ*pir*	λ*pir* derivative of DH5α	(101)
Vibrio fischeri		
ES114	Wild-type isolate from *Euprymna scolopes* light organ	(79)
KL3	ES114 Δ*bsrV*	This study
AKD200	ES114 mini-Tn7 insertion; *camR*	(28, 106)
Select Plasmids[b]		
pCR-BluntII-TOPO	*ori*$V_{ColE1,}$ *kanR*	Invitrogen
pEVS104	CC118 *λ pir* conjugative helper plasmid, *ori*$V_{R6K\lambda}$, *oriT*$_{RP4}$, *kanR, lacZα*	(83)
pVSV105	Conjugative helper plasmid, *ori*$V_{R6K\lambda}$, *ori*V_{pES213}, *oriT*$_{RP4,}$ *camR, lacZα*	(83)
pEVS118	*ori*VR6Kλ, *oriT*$_{RP4,}$ *camR*	(101)
pRMJ13	Downstream region and upstream region of Vf_0735 (*bsrV*) cloned into Blunt-II-TOPO.	R.M. Jones
pRMJ14	Fusion of pRMJ13 and pEVS118 to form Δ*bsrV* allele	R.M. Jones
pKAL4	*bsrV* from ES114 cloned into pCR-Blunt II-TOPO	This study
pKAL6	*bsrV* from ES114 subcloned into pVSV105	This study
Oligonucleotides[c]		
RJ14	GGGTCATCATGCAGTAGCGA	R.M. Jones
RJ28	AATGTCGACCATAAACAACCGTTTTTATATAATAATTATTTCG	R.M. Jones
RJ29	ATTGTCGACTAGACGTCGGGTTGCACCAATTTA	R.M. Jones
RJ30	TAAAAACCGTTTTCATAAAGGAGATTCTTG	R.M. Jones
MNC22	GGTTAAAAAAACGACGATATATAATTCCC	M. Coppinger
MNC23	GTACCTAATTATTCTTACTTAAATTGGTGC	M. Coppinger
KAL1	CATGCTAGCGGTTAAAAAAACGACGATATATAATTCCC	This study
KAL2	CATGCTAGCGTACCTAATTATTCTTACTTAAATTGGTGC	This study

[a]Drug resistance abbreviations used: *camR*, chloramphenicol resistance (*cat*); *kanR,* kanamycin resistance (*aph)*.

[b]Strain ES114 was the source of sequences cloned from *V. fischeri*. Replication origin(s) (*oriV*) on each vector are listed as R6Kγ, ColE1, and/or pES213. Plasmids based on pES213 are stable in *V. fischeri* and do not require antibiotic selection for maintenance (Dunn 2006).
[c]All oligonucleotides are shown in the 5' to 3' orientation. Underlined regions highlight restriction enzyme recognition sites added to facilitate cloning.

Bioinformatic analysis of BsrV. Gene sequences for *bsrV* and *alr* in different bacteria were found by querying the sequences for $BsrV_{Vc}$ (VC1312) and/or $BsrV_{Vf}$ (Vf_0735) against the KEGG genome database, and also by using keywords "Bsr" and "Alr" to search annotations within that database (107, 108). Potential inverted repeats and terminators were investigated using either TransTermHP predictions based on whole genomes or with Pattern Locator (109, 110). Signal peptide predictions were made using SignalP-5.0 (111). Geneious 10.2.6 was used to generate a phylogenetic tree of BsrV and Alr homologs as well as to determine percent similarity from sequence alignments (www.geneious.com). SyntTax was used to assess conserved gene location of BsrV orthologs (112).

Assay for D-amino acids. The strains ES114 (wild type) and KL3 (*bsrV* mutant) along with both strains containing plasmids pVSV105 (control vector) and pKAL6 (*bsrV* in pVSV105) were grown in 25 mL of LBS or minimal medium in 125 mL flasks shaking (200 RPM) at 28°C. Samples were collected at 0 h, 3-6 h (mid-log phase), and 27 h (stationary phase), pelleted, and supernatants were filtered using 0.22 μM filters. These filtrates were assayed for concentration of D-amino acids using the Total D-amino acid assay kit using manufacturer instructions (BioVision, Milpitas, CA). The assay uses D-amino acid oxidase, which produces H_2O_2 upon oxidizing D-amino acids, and fluorogenic detection of H_2O_2 to indirectly quantify D-amino acids.

Growth measurements. Bacterial growth was assessed by adjusting dense cultures to an optical density of 1.0 at 600 nm (OD_{600}) and subculturing (1:100 or 1:1000) into 200 μL of fresh medium in 96-well plates. Cultures were grown shaking (200 RPM) at 28°C, and the OD_{600} was

measured every hour using a BioTek Synergy 2 plate reader (BioTek, Winooski, VT). To assess growth in low-salt media, strains were grown first in LBS, then subcultured into LBS modified to contain the designated concentration of NaCl ranging from 30 mM to 400 mM. Unmodified LBS contains 342 mM NaCl.

PG preparation and analysis. Strains were grown to stationary phase overnight (~20-24 h) with shaking (200 RPM) at 28°C in 400 mL of media in 2L flasks. The samples were then chilled on ice for 10 min and centrifuged at 4°C at 10,000 x g for 15 minutes. Pellets were resuspended in 4 mL of cold water, cell suspensions were dripped into 50 mL boiling 4% SDS with continuous stirring, boiled for 30 min, and the resulting solution allowed to cool to room temperature. Samples were then centrifuged at 130,000 x g for 60 min at room temperature, superanatants discarded, and the pellet resuspended in 15 mL water. Centrifugation at 130,000 x g for 60 min and washing in 15 mL water was repeated until SDS was undetectable. Detection of SDS in the supernatant was assayed using methylene blue and chloroform (113). The final peptidoglycan pellet was resuspended in 1 mL of water and stored at -20°C. Amino acid and muropeptide analyses were performed by our collaborator Dr. David Popham (Virginia Tech) using HPLC as previously described (114).

Squid colonization. *E. scolopes* juvenile squid were inoculated with individual *V. fischeri* strains, ES114 (wild-type) or KL3 (Δ*bsrV*), within 4 h of hatching as previously described (94). The *V. fischeri* strains were grown in ASWT to an OD_{600} of 0.3-0.7 and diluted in Instant Ocean (United Pet Group Inc., Cincinnati, OH) to achieve between ~1000-2000 CFU/mL, then was plated on LBS to determine the actual inoculum density, which was similar for each strain in each experiment. Between 4 and 20 squid were added to 100 mL of filter-sterilized Instant Ocean® and then inoculated with either a strain of interest or no bacteria as an aposybiotic control. Water was

replaced with fresh filter-sterilized Instant Ocean every 12-24 h. After 48 h post-inoculation, squid were homogenized and the homogenates were serially diluted and plated to determine CFU per squid.

Mutant competitiveness was tested using competitive colonization assays where squid that had hatched between 4 h – 24 h were exposed to a ~1:1 ratio of AKD200 (ES114 with a chloramphenicol marker that does not appear to affect fitness) and KL3 (Δ*bsrV*) which each had been grown to an OD_{600} between 0.3 and 0.7. Water was replaced with fresh filter-sterilized every 12-24 h, and the squid were collected after 48 h infection. Squid were then homogenized, serially diluted, plated, and finally patched to LBS plates supplemented with chloramphenicol to determine the ratio of AKD200 to KL3. The relative competitiveness index (RCI) was determined by dividing KL3 to AKD200 ratio in each individual squid by the ratio of these strains in initial inoculum. Average RCI and statistical significance were calculated using log-transformed data. An RCI < 1 indicates the mutant strain was outcompeted by the wild-type, an RCI > 1 indicates the wild-type was outcompeted by the mutant, and an RCI = 1 indicates no competitive difference between the strains.

Competition in mixed cultures. KL3 (Δ*bsrV*) was competed against the *camR*-marked strain AKD200 (see competitiveness assays in squid above). Individual strains were grown to mid-log phase (OD_{600}= 1.5), mixed ~1:1, and the culture was dilution plated and patched onto plates with chloramphenicol to determine the starting ratio of KL3 and AKD200. The mixed co-culture was subcultured 2^{10}-fold and regrown to a similar OD_{600} to achieve ten generations of growth. An aliquot of the culture was then serially diluted and plated on LBS. The following day colonies were patched to LBS plates with and without chloramphenicol supplementation to determine the strain ratio after ten generations. The process of subculturing, regrowth, plating, and patching was

repeated for later generations. The RCI of the mutant strain was calculated as described above. ES114, the unmarked wild-type strain, was also competed against AKD200 using this method as a control to test whether the *camR* marker in AKD200 affected fitness.

RESULTS

Bioinformatic analysis of BsrV homologs in *Vibrio* species. Previous studies indicated *bsrV* is found in other bacteria (15), and our query of updated databases confirmed and extended those results. *Vibrio mimicus,* a closely related species to *V. cholerae*, contains a $BsrV_{Vc}$ homolog with 99% protein similarity to $BsrV_{Vc}$, while the BsrV encoded by *V. fischeri*, $BsrV_{Vf}$, exhibits only 85% protein similarity to $BsrV_{Vc}$. Many *Vibrio* species have protein sequence similarity between 90 to 99% to $BsrV_{Vc}$, including *V. alginolyticus, V. antiquaries, V. diabolicus, V. furnissii, V. vulnificus,* and *V. coralliilyticus.* When presented in a tree constructed based on protein sequence, the BsrV homologs from these organisms cluster more closely to the archetypal BsrV of *V. cholerae* than to $BsrV_{Vf}$ (Figure 2.1). The BsrV homologs that most closely align with $BsrV_{Vf}$ are encoded in the genomes of *V. wodanis*, *V. logei*, and *V. finisterrensis*, each of which have a BsrV ortholog with 90 to 99% sequence similarity to $BsrV_{Vf}$ (Figure 2.1). This analysis indicates that there are two distinct lineages of BsrV orthologs and these genetic differences may confer differences is function and cellular role.

BsrV belongs to the alanine racemase protein family, and one might expect homology searches with BsrV to return proteins that are alanine-specific racemases (Alr), which are widespread and used for the D-Ala biosynthesis required in PG biosynthesis. To gain perspective into the degree of relatedness between the putative broad-spectrum racemases (BsrVs) above relative to $BsrV_{Vc}$ or to the more common alanine racemases, we included Alr sequences in our

analysis. As reported previously, the protein identity between $BsrV_{Vc}$ and this bacterium's Alr racemase is around 28%. This trend is consistent with small differences in all *Vibrio* species that contain both a BsrV ortholog and Alr (15). Moreover, despite belonging to the same family of racemases, the proteins annotated as Alr and BsrV clearly cluster distinctly from each (Figure 2.1).

Enzymatically similar broad-spectrum racemases from bacteria outside the *Vibrionaceae* were also included in this analysis. The Bsr's from *P. mirabilis, P. putida*, and *P. taetrolens* cluster together and appear distinct from the Bsr's found in the *Vibrionaceae* (Figure 2.1) and are no more closely related to $BsrV_{Vc}$ or $BsrV_{Vf}$. The two racemases with broad substrate specificity in the Gram-positive bacterium *O. oeni* appear as their own cluster and were as related to the enzymatically specific Alr's as to the other Bsr's investigated (Figure 2.1).

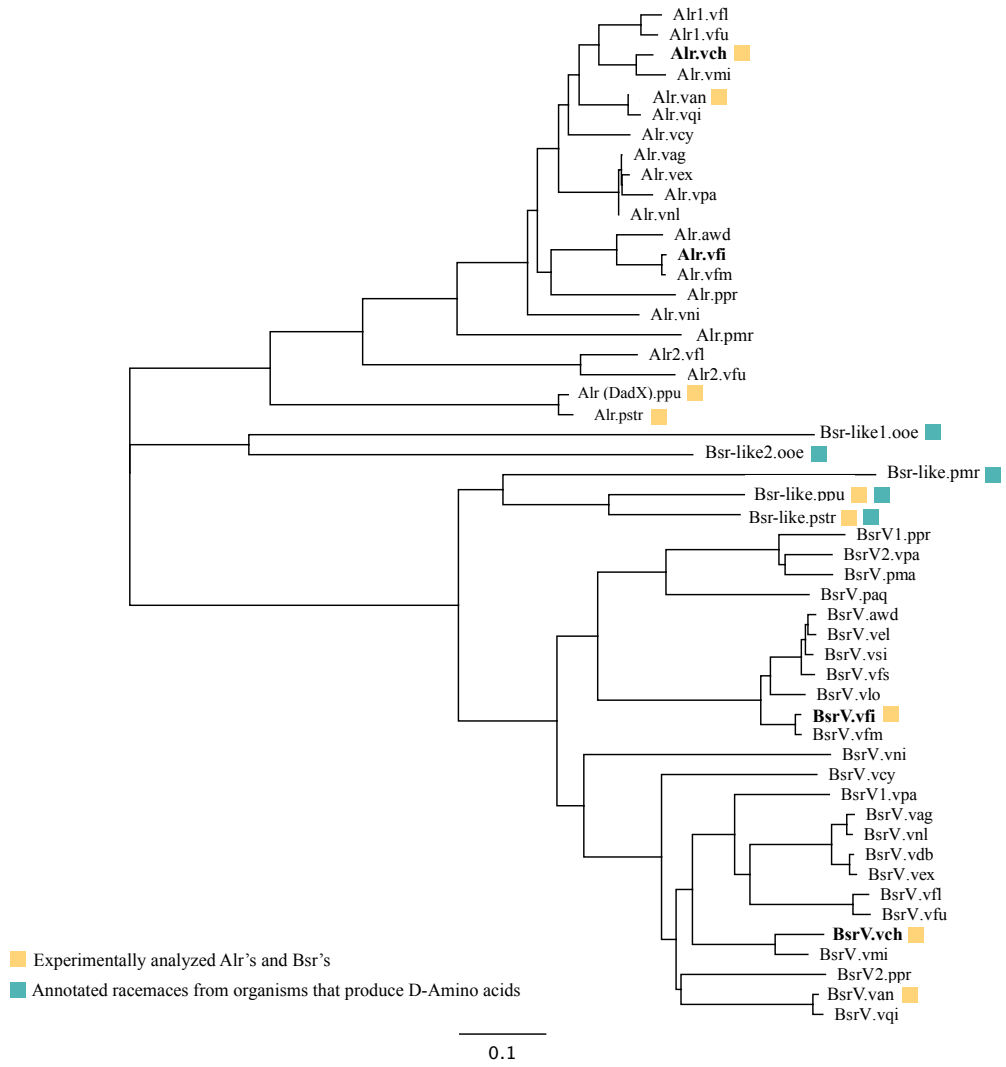

Figure 2.1. Phylogenetic tree of BsrV and Alr homologs within the *Vibrionaceae* family and other organisms. (Top) Alr homologs from various species. (Bottom) Bsr and BsrV homologs from various species. Alr and BsrV homologs from *V. fischeri* and *V. cholerae* are distinguished in bold text (BsrV.vfi and BsrV.vch respectively). The scale bar indicates 0.1 amino acid substitutions per site. Proteins marked with an asterisk are Bsr's enzymatically similar to BsrV and contained within non-*Vibrio*-related species. Species are abbreviated as *V. fischeri* ES114 (Vfi), *V. wodanis* (Awd), *V. cholerae* (Vch), *V. parahaemolyticus* (Vpa), *V. alginolyticus* (Vag), *V. antiquaries* (Vex), *V. diabolicus* (Vdb), *V. furnissii,* (Vfu), *V. nigripulchritudo* (Vni), *V. anguillarum* (Van), *V. coralliilyticus* (Vcy), *V. mimicus* (Vmi), *V. qinghaiensis* (Vqi), *V. neocaledonicus* (Vnl), *V. vulnificus* (Vvu),*V. fluvialis* (Vfl), *Photobacterium profundum* (Ppr), *V. logei* (Vlo), *V. finisterrensis* (Vfn), *V. sifiae* (Vsi), *V.* EL58 (Vel), *Photobacterium aquae* (Paq), *Photobacterium marinum* (Pma), *P. mirabilis* (Pmr), *O. oeni* (Ooe), *P. putida* (Ppu), *P. taetrolens* (Pstr).

In *V. cholerae*, $BsrV_{Vc}$ was reported to be a periplasmic protein, and we used SignalP-5.0 (111) to predict whether other BsrVs contained signal peptides that would direct their export. With one exception, all *Vibrionaceae* BsrV orthologs including $BsrV_{Vf}$ have predicted signal peptides, suggesting export from the cytoplasm using the Sec translocon and cleavage by Signal Peptidase I. The one exception was the BsrV encoded by *P. profundum*, which lacked a predicted signal peptide to direct secretion. Like the Bsr orthologs from most *Vibrio* species, the Bsr-like proteins from the non-*Vibrio* species *P. taetrolens, P. putida,* and *P. mirabilis* also have predicted signal peptides, with the latter using a lipoprotein signal peptide to direct transport by the Sec translocon and cleavage by Signal Peptidase II. Neither of the two Gram-positive *O. oeni* Bsr orthologs nor *Vibrionaceae* Alr's contain predicted signal peptides.

Interestingly some notable *Vibrio* species do not encode BsrV homologs at all within their respective genomes, while other members of the *Vibrionaceae* encode two putative BsrV proteins. Examples of *Vibrio* species that do not possess functional BsrV orthologs include *V. salmonicida,* where a transposon interrupts the CDS 290 bp into the gene (Figure 2.2), as well as those that do not contain any evidence of a BsrV ortholog including *V. harveyi, V. profundi, and V. campbellii.* On the other hand, species that contain more than one BsrV homolog include *V. parahaemolyticus* and *Photobacterium profundum,* and in these bacteria one BsrV more closely clusters with $BsrV_{Vc}$ and the other more closely resembles $BsrV_{Vf}$ (Figure 2.1).

Because gene location and context can provide clues for function and evolutionary relationships, we investigated the synteny of *bsrV* within *Vibrio* species. $bsrV_{Vf}$ is located between *dinB* and *pepD*, which encode DNA polymerase IV and an aminoacyl-histidine dipeptidase, respectively. This arrangement of genes around $bsrV_{Vf}$ (Figure 2.2) is only conserved among the species that encode BsrV orthologs with the highest identity to $BsrV_{Vf}$, and its context does not

suggest a functional role (Figure 2.1). An alternate genetic configuration was seen for *V. cholerae* and the bacteria encoding the most similar orthologs to BsrV. These bacteria share an arrangement with a gene encoding a methyl-accepting chemotaxis protein upstream of *bsrV* and some variation of an amino acid transport gene downstream (Figure 2.3). The genes encoding methyl-accepting chemotaxis proteins found upstream of *bsrV's* in $BsrV_{Vc}$-like organisms appear to contain a Tar-/Tsr- domain which, in related chemoreceptors in *E. coli* allows for chemotaxis towards Asp and Ser, respectively (115). The transporters encoded downstream of $bsrV_{Vc}$ appear to be permeases involved in amino acid transport. This co-localization of *bsrV* with proteins involved in amino acid transport and chemotaxis may be clues into BsrV's functional role for the cells. Further downstream of *V. cholerae*-like *bsrV's*, is a TyrR-type transcriptional regulator. While BsrV is unable to act *in vitro* on Tyr or other aromatic amino acids (15), this putative regulator may control the transcriptional regulation of either bsrV or nearby genes related to amino acid transport and chemotaxis. *P. profundum* and *V. fluvialis* contain *bsrV* in distinct genetic arrangements (data not shown).

During this study, we had significant difficulty PCR amplifying across $bsrV_{Vf}$ in order to distinguish clones with the Δ*bsrV* allele. Upon investigating the genome sequence for insight into this obstacle, we found a pair of 37-bp inverted repeats (74 bp total) located 44 bp after the stop codon of *bsrV* where the reverse primers we initially tried for confirmatory PCR would bind (109). After changing the PCR protocol to include a reverse primer that binds between the BsrV CDS and the inverted repeat, we were able to successfully amplify *bsrV* with colony PCR or purified genomic DNA as template to confirm allelic exchange during strain construction (see Materials and Methods). We then sought to determine if this genomic feature is unique to $bsrV_{Vf}$ or if it is conserved in other *Vibrio* species. We found that some other *Vibrio* species, including

V. cholerae, *V. furnissi* and *V. vulnificus* contain inverted repeats at least 55-bp in length either before or after *bsrV*, such as *V. furnissi* and *V. vulnificus*. In *V. cholerae*, each repeat is 36 bp, which is approximately the same length as those found in *V. fischeri*, but its location is immediately before the CDS of *bsrV* and shares no apparent sequence identity with the repeat found in *V. fischeri* (Figure 2.2 & 2.3).

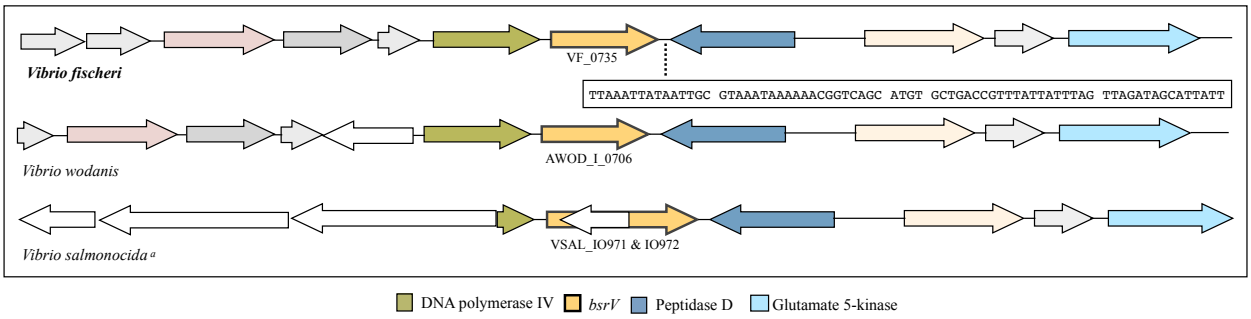

Figure 2.2. Synteny of *V. fischeri*-like *bsrV* homologs. *bsrV* homologs (yellow arrows) in *V. fischeri* (bold, VF_0735), *V. wodanis* (AWOD_I_0706), and *V. salmonocida* (VSAL_IO971) are contained between *dinB* (green arrows) and *pepD* (blue arrows), which encode DNA polymerase IV and peptidase D, respectively. The *bsrV* homolog in *V. salmonocida* (VSAL_IO971) is interrupted by a transposase insertion (VSAL_IO972). The gene which encodes ProB, a glutamate kinase (light blue arrows), is found downstream of these *bsrV* homologs. A large inverted repeat (boxed sequence) was discovered downstream of *bsrV* in *V. fischeri* using TransTermHP and Pattern Locator.

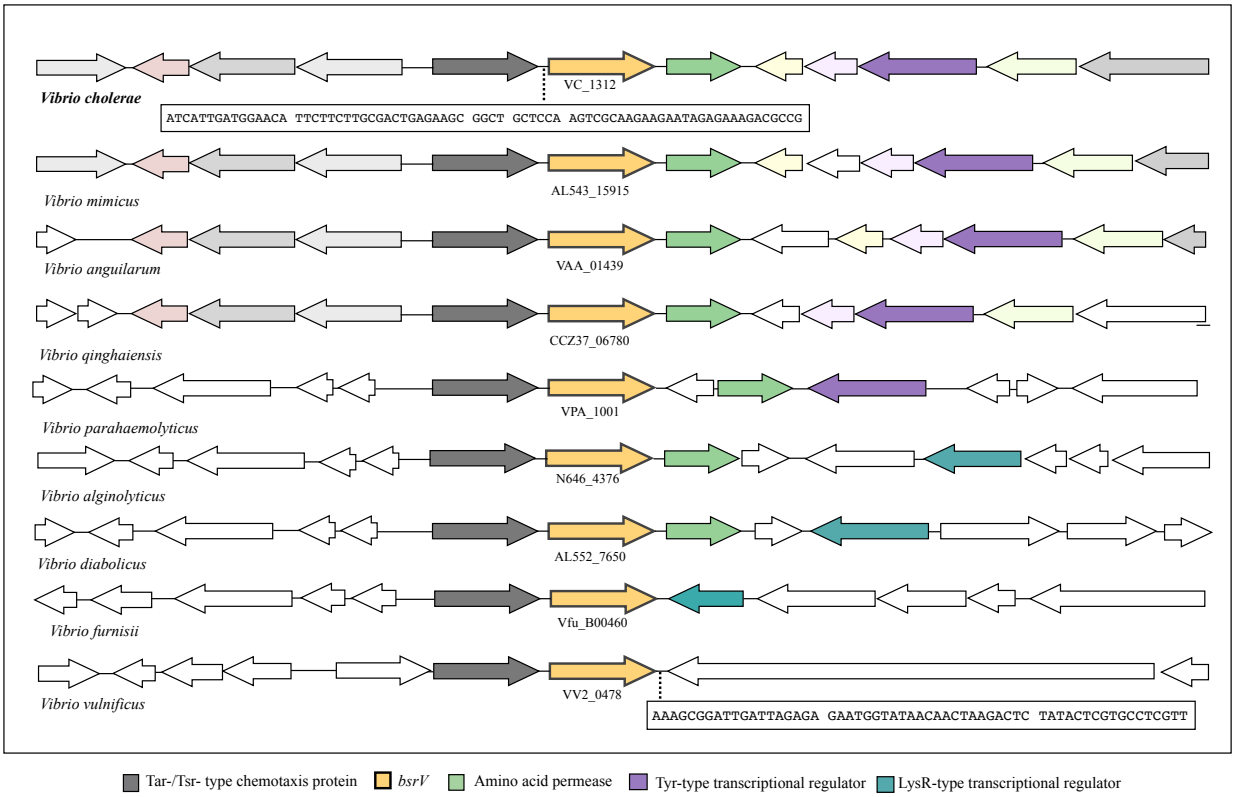

Figure 2.3. Synteny of *V. cholerae*-like *bsrV* homologs. *bsrV* homologs (yellow arrows) in *V. cholerae* (bold, VC_1312), *V. mimicus* (AL543_15915), *V. anguilarum* (VAA_01439), *V. qinhaiensis* (CCZ37_06780), and *V. diabolicus* (AL552_7650) are contained between a Tar-/Tsr-type chemotaxis protein (gray arrows) and an amino acid permease (green arrows). *bsrV* homologs in *V. cholerae*, *V. mimicus, V. anguilarum, V. qinqhaiensis,* and *V. parahaemolyticus* are all upstream of a Tyr-type transcriptional regulator (purple arrows) while *V. alginolyticus, V. diabolicus, V. furnisii* (Vfu_B00460), and *V. vulnificus* (VV2_0478) are all upstream of a LysR-type transcriptional regulator (blue arrows). Large inverted repeats (boxed sequences) were discovered *V. cholerae* (upstream of *bsrV*) and *V. vulnificus* (downstream of *bsrV*) using TransTermHP and Pattern Locator.

BsrV is responsible for the production of D-amino acids in *V. fischeri* supernatants.

To determine if BsrV is responsible for D-amino acid production in *V. fischeri*, the concentration of D-amino acids was assayed in the supernatants of the wild type and the *bsrV* mutant along with both strains containing plasmids pVSV105 (control vector) and pKAL6 (*bsrV* in pVSV105). The assay relies on D-amino acid oxidase, which produces H_2O_2 upon oxidizing D-amino acids, and fluorogenic detection of H_2O_2 to indirectly quantify D-amino acids. First, we assayed supernatants

after 20 h of growth in LBS medium and found that D-amino acid content in supernatants of the *bsrV* mutant contained an amount of D-amino acids three orders of magnitude lower than supernatants of the wild-type parent and not significantly above background (data not shown) (Figure 2.4). When *bsrV* is provided *in trans* on a plasmid in the *bsrV* mutant, D-amino acid production was restored to wild-type levels (Figure 2.4, solid bars). However, when the wild-type and *bsrV* mutant were grown to similar densities for 24 h in minimal medium, which does not contain any exogenous L- or D-amino acids, accumulation of D-amino acids in the culture was not significantly above background for either the wild-type or the *bsrV* mutant (Figure 2.4, Striped bars).

To determine how growth phase influenced D-amino acid production, we tested the amount of D-amino acid in the spent media of the wild type and the *bsrV* mutant over the course of growing a batch culture. Although the standard error was large in these experiments, the results indicate that *V. fischeri* produced D-amino acids throughout growth, rather than being restricted to stationary phase, as was the case in *V. cholerae* (13). Consistent with the results in Figure 2.4, the *bsrV* mutant produced significantly less D-amino acids than the wild-type (Table 2.2).

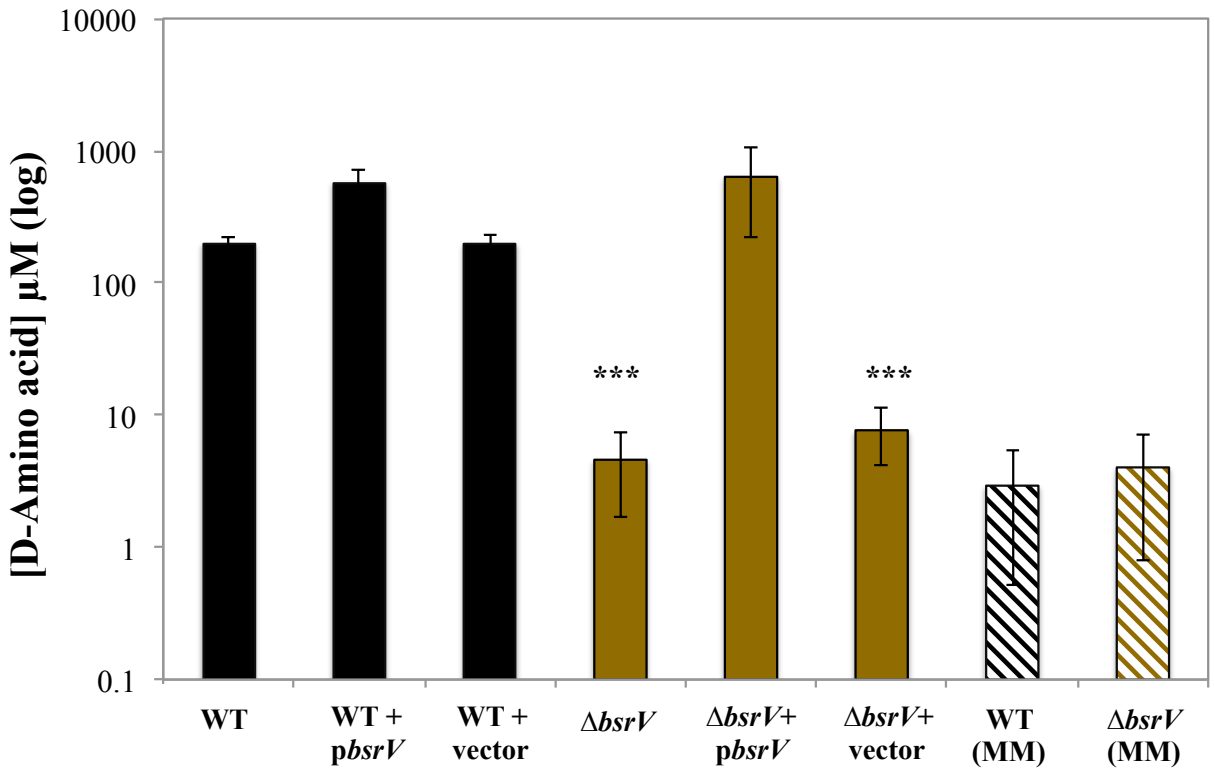

Figure 2.4. *bsrV*-dependent production of D-amino acids in *V. fischeri*. (Solid bars) D-amino acids were measured in culture supernatants of ES114 (wild-type) and KL3 (Δ*bsrV*) along with both strains containing plasmids pVSV105 (control vector) and pKAL6 (*bsrV* in pVSV105) grown in LBS for 20 h at 28°C. (Striped bars) D-amino acids were measured in culture supernatants of ES114 (wild type) and KL3 (Δ*bsrV*) grown in a defined minimal medium for 24 h at 28°C. Values shown are the averages of three experiments. Error bars indicate standard error. Values marked with asterisks indicates a significant difference relative to ES114 grown under the same conditions as determined by a Student's T-test (Student's T Test - $p<0.0002$).

Table 2.2. *bsrV*-dependent D-amino acid production in *V. fischeri* during active growth

	ES114 (wild type)		KL3 (Δ*bsrV*)	
Time (hr)	**OD600**	**[D-amino acid] µM[a]**	**OD6002**	**[D-amino acid] µM**
0	0.0	10 [+/- 8]	0.0	0 [+/- 4]
3	0.3	189 [+/- 99]	0.3	1 [+/- 5]
5	1.7	451 [+/- 360]	1.6	5 [+/- 4]
6	3.2	258 [+/- 70]	2.9	18* [+/- 15]
27	9.3	110 [+/- 27]	9.8	0* [+/- 3]

[a][D-amino acid] was measured in the supernatant of growing cultures using the fluorogenic total D-amino acid assay kit (BioVision, see Materials and Methods). Data represent the combined results of three independent assays, standard deviation is represented within brackets. Values marked with an asterisk indicate the concentration of D-amino acids was significantly different than that of the wild-type ($p<0.05$).

Altered PG observed in *V. fischeri* mutants lacking *bsrV*. Next, we investigated the PG structure in the *bsrV* mutant. PG from stationary phase cultures of ES114 (wild type) and KL3 (*bsrV* mutant) and the mutant containing *bsrV* in trans (pKAL6) was isolated and analyzed via Reverse Phase HPLC. Analysis of muramidase-digested PG yielded two peaks (p1 & p2) in the wild type and the complemented strain that were absent in the *bsrV* mutant (Figure 2.5A-C). The compounds associated with these fractions were then analyzed by mass spectrometry (MS). Notably, many of the muropeptides contain anhydroNAM, which is a product of lytic transglycosylases that digest PG during changes in cell shape (116). This prevalence of anhydroNAM may be due to the PG being from stationary phase cultures, which have been undergoing reductive division to yield smaller cell size. Peak p2, which is absent in the *bsrV* mutant, gives a mass that is expected for a muropeptide containing Met in place of Ala (Figure 2.5D and F). This substitution was observed previously in both *V. cholerae* and *Escherichia coli* wild-type stationary phase PG when cells were grown in the presence of exogenous D-Met (13, 31). Usually, additional fragmentation of the muropeptides will cause a loss and separation of D-Ala from the muropeptide, which can be observed through MS analysis. Curiously, additional fragmentation of p2 did not result in an analogous loss of D-Met, which may indicate that D-Met, or whatever has been substituted at this position, is not as subject to loss as is D-Ala.

MS data for p1, which is also absent in the *bsrV* mutant, appears as a shoulder on a peak corresponding to a normal muropeptide that has a very similar retention time to peaks present in all three strains. However, p1 has a mass 106 Daltons greater than the adjacent conserved peak,

and this mass fragments with the *m*-DAP residue, indicating it is attached to the third position of the peptide (Figure 2.5D and E). Additional fragmentation of peaks and MS analysis is necessary to determine the identities of these muropeptide modifications in p1.

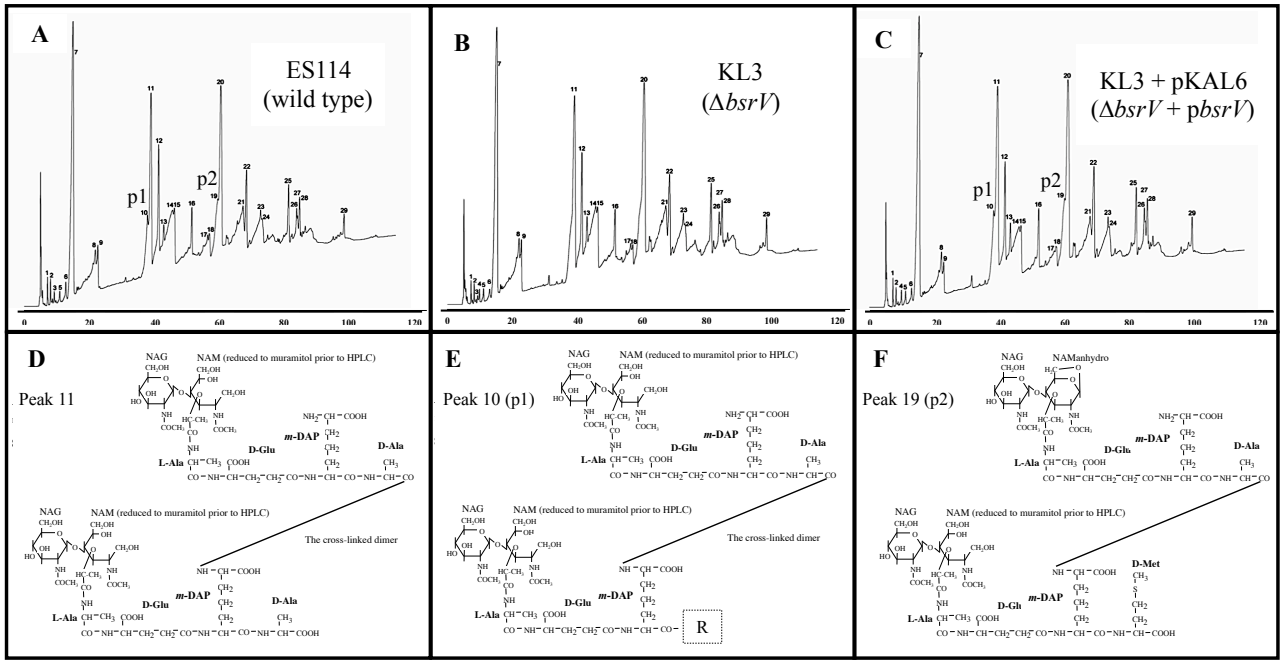

Figure 2.5. Altered peptidoglycan structure in *bsrV* mutant in *V. fischeri.* (A-C) Reverse Phase-HPLC analysis of stationary phase peptidoglycan from ES114 (wild-type), KL3 (Δ*bsrV*), and KL3 + pKAL6 (Δ*bsrV* with wild-type *bsrV* on a low-copy plasmid in trans). (D) Peak 11, a canonical muropeptide found in stationary phase peptidoglycan of all strains. It's predicted structure is NAG-NAM_{OH} ~ Ala-Glu-*m*-DAP-Ala ~ Ala-Glu-*m*-DAP-**Ala** ~ NAG-NAM_{OH}. (E) Peak 10, an altered muropeptide absent in the *bsrV* mutant and found only in stationary phase peptidoglycan of ES114 and KL3 + pKAL6. The predicted structure is NAG-NAM_{OH} ~ Ala-Glu-*m*-DAP-Ala ~ Ala-Glu-*m*-DAP-**R** ~ anhydro-*N*-acetylmuramic acid, where **R** is an unknown 177-Dalton moiety (dashed box). (F) Peak 19, an altered muropeptide absent in the *bsrV* mutant and found only in stationary phase peptidoglycan of ES114 and KL3 + pKAL6. The predicted structure is NAG-NAM_{OH} ~ Ala-Glu-*m*-DAP-Ala ~ Ala-Glu-*m*-DAP-**Met** ~ anhydro-*N*-acetylmuramic acid. All predicted structures (D-F) based on mass spectrometry analysis courtesy of collaborator Dr. David Popham.

***V. fischeri* mutant lacking *bsrV* is less tolerant to low-salt conditions.** A *V. cholerae* *bsrV* mutant was three-fold more sensitive to osmotic challenge, and we tested if this effect

occurred in *V. fischeri* (13). The *V. fischeri* strains ES114 (wild type) and KL3 (*bsrV* mutant) along with both strains containing plasmids pVSV105 (control vector) and pKAL6 (*bsrV* in pVSV105) were grown in rich medium (LBS) with variable salt concentrations for 24 h. At low NaCl concentrations, between 30-50 mM NaCl, the *bsrV* mutant showed decreased growth compared to the wild type, and the presence of *bsrV in trans* restored growth approximately to wild-type levels (Figure 2.6). Above 60 mM NaCl, there were no observable differences between the mutant and the wild type. This result is consistent with the low-salt sensitivity of a *V. cholerae bsrV* mutant, although in that study osmotolerance was measured as survival after an osmotic challenge only in stationary phase (13).

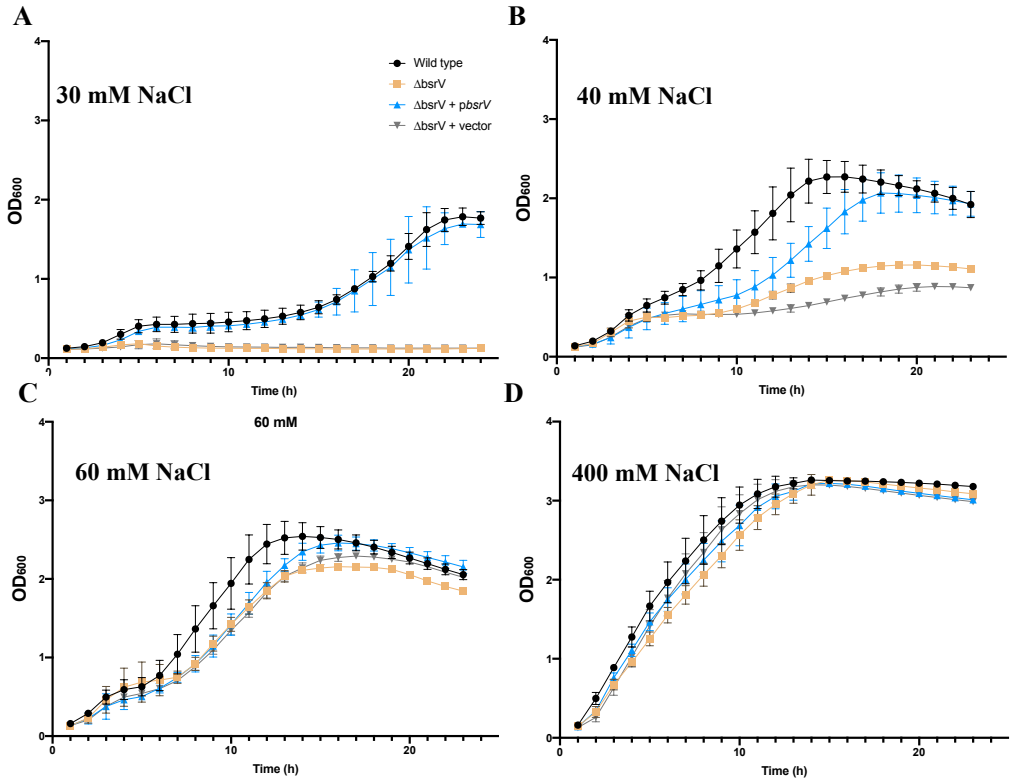

Figure 2.6. *bsrV* mutant exhibits decreased tolerance to low-salt media compared to wild-type. ES114 (wild-type, black), KL3 (Δ*bsrV,* yellow), KL3 + pKAL6 (Δ*bsrV* + p*bsrV,* blue), and KL3 + pVSV105 (Δ*bsrV* + control vector, brown) were grown in LBS with varying [NaCl] to test tolerance in low salt environments. (A) Growth of strains in 30 mM NaCl LBS, (B) Growth of strains in 40 mM NaCl LBS, (C) Growth of strains in 60 mM NaCl LBS, and (D) 400 mM NaCl LBS. Strains were grown for 6 h, and sub-cultured into 200 uL of indicated LBS medium in a 96-

well plate, grown for 24 h shaking (200 RPM) at 28°C, and OD_{600} was measured every hour. Values shown are averages of three experiments and error bars indicate standard error.

BsrV is not essential for light-organ colonization in the *Vibrio-Euprymna* symbiosis. We tested whether BsrV contributes to ES114's ability to establish symbiotic infection and found that the *bsrV* mutant had no obvious defect in colonization of the squid for the first 48 h of infection (Figure 2.7A). Some subtle colonization defects are only evident during competition, and competition experiments have the advantages that strains colonize the same animals, eliminating error due to animal to animal variability (117, 118). To test the mutant's competitiveness, it and a chloramphenicol-resistant derivative of ES114 (AKD200) were mixed ~1:1 and exposed to the squid over 48 h. The marker in AKD200 is convenient for determining strain ratios but does not appear to affect symbiotic fitness (117). The ratio of the strains within the *E. scolopes* light organ was determined on the second day after the infection. We found that like the single-strain inoculation, the colonization competitiveness was similar for both AKD200 and the *bsrV* mutant (Figure 2.7B). These findings illustrate that BsrV is not necessary to infect *E. scolopes* and does not play an apparent role during the first 48 hours of colonization.

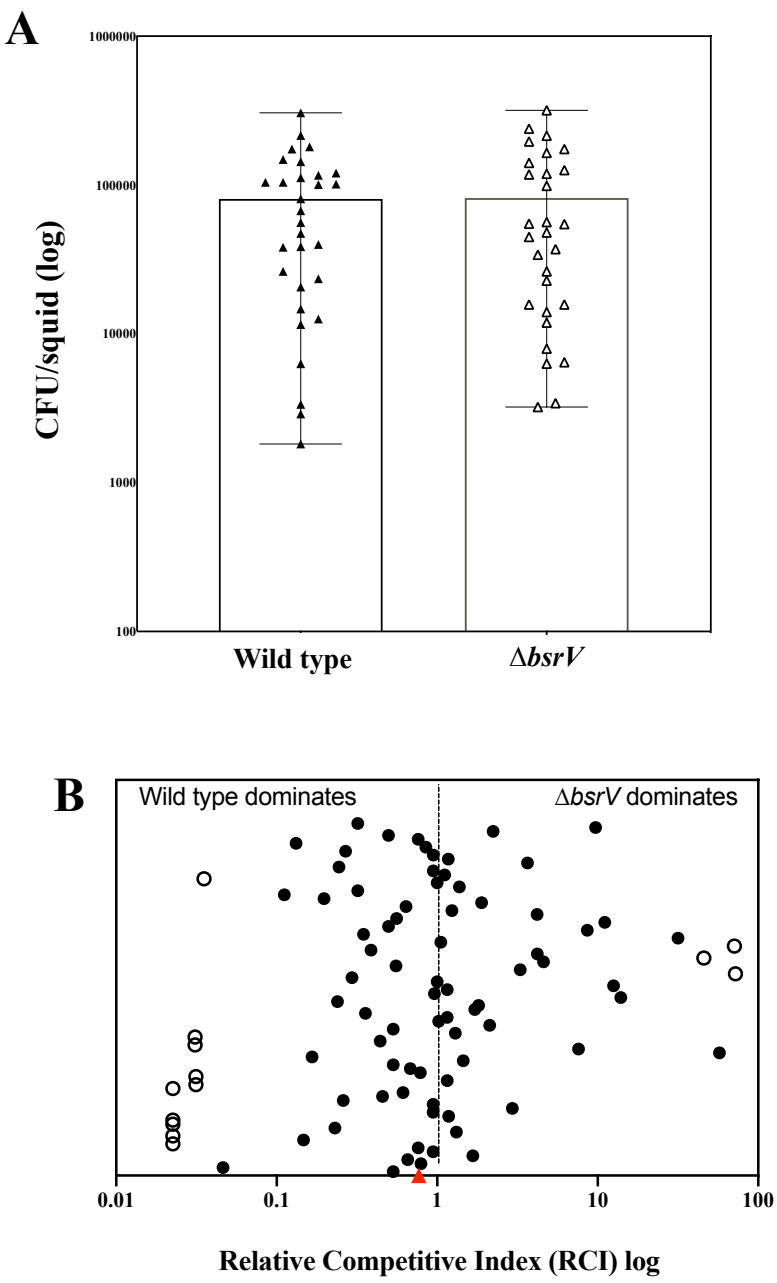

Figure 2.7. Colonization of *E. scolopes* by *bsrV* mutant and wild type. (A) Average colonization levels in CFU *V. fischeri* per squid 48 h after inoculation with wild-type (ES114; solid triangles, left bar) and Δ*bsrV* (KL3; open triangles, right bar). Treatments are not significantly different (p=0.427). Bars indicate the standard deviation (n= 30 for wild-type and 29 for Δ*bsrV*). (B) Relative competitiveness between AKD200 (a *camR*-marked ES114) and *bsrV* mutant (KL3) during colonization of *E. scolopes.* Juvenile squid exposed to a mixed (~1:1) inoculum of wild-type and mutant, and the relative competitiveness was determined after 48 h infection. Circles represent the relative competitiveness index (RCI) in each infected animal (n=89). Open circles

represent animals that were singly infected by one strain with the other below the limit of detection. The red triangle represents the average RCI (0.7675).

The *V. fischeri bsrV* mutant out-competes wild type in culture. We also investigated the competitive fitness of the *bsrV* mutant in culture. We competed KL3 (*bsrV* mutant) against the marked-competitor strain AKD200 starting from a ~1:1 inoculum ratio in LBS medium and found that over time, the *bsrV* mutant consistently outcompeted AKD200 with the average RCI greater than 1 and a 6.06% fitness advantage per generation (Figure 2.8, solid triangles). This surprising result prompted us to test if AKD200 (mini-Tn7 CmR) was outcompeted due to the resistance marker. To test this possibility, we competed the wild-type strain ES114, which was the parent for both KL3 and AKD200, against AKD200. We found that over 50 generations ES114 did not have any fitness advantage over AKD200 (Figure 2.8, open circles). This validates our finding that the *bsrV* mutant outcompetes wild type in culture.

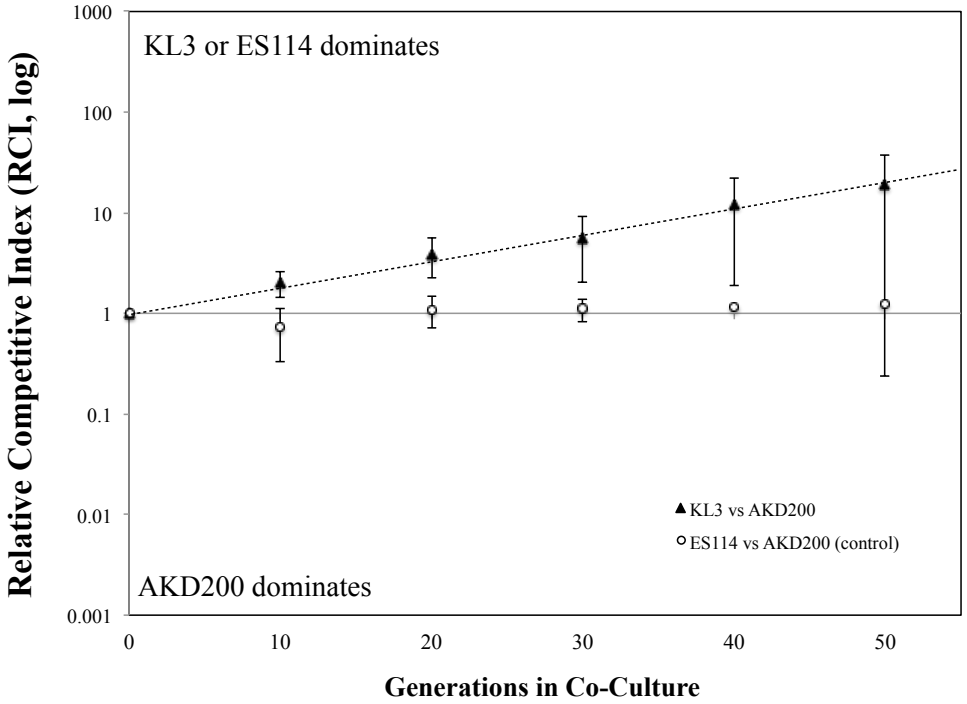

Figure 2.8. *V. fischeri bsrV* mutant outcompetes wild type in culture. (Triangles) To determine the relative fitness of KL3 (Δ*bsrV*) compared to wild-type, KL3 was co-cultured with AKD200

(wild-type, mini-Tn7 CmR) with an initial ~1:1 ratio. Every 10 generations the relative competitive index was determined through the ratio KL3 to AKD200. Values represent averages of three experiments and error bars are standard error. (Open circles) ES114 (laboratory wild-type strain) was competed against AKD200 (mini-Tn7 CmR) to determine validity of using AKD200 as a wild-type strain. Strains were initially co-inoculated in a ~1:1 ratio, and every 10 generations the relative competitive index was determined through the ratio of ES114 to AKD200. Values represent averages of biological replicates in one experiment and error bars are standard error. A linear regression on logarithmic data yields a slope 1.0602, indicating a 6% fitness advantage per generation with an $R^2 = 0.99$.

DISCUSSION

Over the past two decades, NCDAA production by BsrV has been of considerable interest in the pathogenic organism, *V. cholerae* (5, 13-15). As many Vibrio species contain BsrV orthologs, we sought to investigate the roles of the racemase in a closely related organism, *V. fischeri. V. fischeri* is a model organism that is not only safer to study as a BSL-1 organism, but also participates in a unique, mutualistic relationship; the light-organ symbiosis between *V. fischeri* and *E. scolopes* (86). Here, we show that BsrV orthologs are found in the genomes of diverse *Vibrio* species and report the physiological similarities and differences between the role of BsrV in *V. fischeri* and the more extensively studied $BsrV_{Vc}$ in *V. cholerae.* In addition to previously reported functions of BsrV in increased resistance to osmotic stress, we found that it played no discernible role during establishment of the *Vibrio-Euprymna* mutualism, and it carried some fitness cost during growth in LBS medium.

Because diverse organisms produce NCDAAs and contain BsrV homologs (13, 15), we sought to more closely investigate the relatedness of orthologs, gene context, and gene structure of *bsrV*'s within *Vibrio* species. Our findings suggest that BsrV is conserved among many but not all *Vibrio*s. Based on protein similarity, the BsrV orthologs within the *Vibrionanceae* can be divided into two main groups, one represented by *V. cholerae* BsrV and the other by *V. fischeri*

BsrV (Figure 2.1-2.3). Many of the *bsrV*'s that are more similar to the *V. cholerae* ortholog are localized near amino acid transporters and chemotaxis proteins, providing some clue into BsrV's role with respect to D-amino acid production (Figure 2.3). Interestingly, *V. parahaemolyticus* (vpa), *Photobacterium profundum* (ppr) contain two BsrV homologs, one in each of these protein clusters (Figure 2.1). The enzymatically similar Bsr's from non-*Vibrio* species such as *P. mirabilis, P. putida*, and *P. taetrolens* appear to be more related to the orthologs of each other than to those contained within *Vibrio* species. We suspect that the sequence differences between BsrVs may be reflected by functional differences and contribute to the subtly distinct roles we observed for $BsrV_{Vf}$ and $BsrV_{Vc}$.

In *V. cholerae*, BsrV is the primary producer of NCDAAs, such as D-Met and D-Leu, during stationary phase. These are incorporated into the PG of stationary phase cells (13). Here, we report that BsrV in *V. fischeri* is similarly responsible for D-amino acid accumulation in supernatants of stationary phase cultures (Figure 2.4). However, we observed that D-amino acid production is not a uniquely stationary phase phenomenon. Rather, we report evidence that BsrV produces D-amino acids during active growth (Table 2.2). We also found that neither the wild type nor *bsrV* mutant produced D-amino acids above background levels when grown to similar densities in minimally defined medium, suggesting the presence of a necessary substrate or induction molecule for BsrV in rich medium (LBS). Further work is necessary to elucidate the identity of this unknown and necessary component of LBS for BsrV's function. Future work in *V. fischeri* requires an investigation into the identities of the NCDAAs produced by BsrV during exponential and stationary phase, and a comparison to that of other organisms with *bsrV* orthologs.

Previously, it was hypothesized that the incorporation of BsrV-produced D-amino acids regulates the quantity and strength of the peptidoglycan to ameliorate the stresses that arise during

the transition to stationary phase (13). When previously tested in *V. cholerae*, a *bsrV* mutant was more sensitive to osmotic challenge than the wild type. Osmotolerance was measured through survivability after challenging stationary-phase cells to low-salt conditions, because in *V. cholerae* BsrV expression appeared restricted to stationary phase. We attempted this method for testing osmotolerance in *V. fischeri* but found it yielded inconsistent results (data not shown). Instead, we tested osmotolerance in *V. fischeri* by comparing growth in media with varying salt concentrations. We demonstrated that low-salt conditions caused attenuated growth in the *bsrV* mutant at all growth stages of batch culture (Figure 2.6). The *bsrV* mutant showed growth deficiencies in 30, 40, and 50 mM NaCl but no difference to wild type in $\geq$60 mM NaCl. Thus, in both *V. cholerae* and *V. fischeri*, BsrV appears to play a role in tolerance to osmotic stress, but in *V. fischeri* this phenomenon is not unique to stationary phase (4).

One way that D-amino acids might contribute to cell wall strength is by their incorporation into PG. Here, we report that as in *V. cholerae* (13), stationary phase PG of wild-type cells has subtly altered muropeptides (Figure 2.5). Two peaks observed in wild-type peptidoglycan are missing from the *bsrV* mutant. Based on fragmentation and mass spectrometry data of these peaks, we hypothesize that one of the peaks (p2, Figure 2.5F) represents a muropeptide with D-Met incorporated into the peptide chain in place of D-Ala. The other peak missing from the *bsrV* mutant (p1, Figure 2.5) gives less conclusive fragmentation/MS data. The peak's retention time and mass is very similar to a canonical muropeptide with an additional mass of 106 Daltons. During MS analysis, the unknown, additional 106-Dalton mass fragments with *m*-DAP, indicating that the additional mass is attached to this residue in the peptide (Figure 2.5E). Additional fragmentation does not yield the loss of Ala (70 Daltons), which is common with normal muropeptides. This indicates that the substituted moiety is not as subject to loss as Ala is in a canonical peptide and is

approximately 177 Daltons. The 177-Dalton moiety does not correspond to any known proteinogenic amino acid. It is possible that the incorporation of a non-proteinogenic amino acid or more than one amino acid into the muropeptide occurs in strains that have BsrV, and further investigation is warranted to test this possibility. Growing cells in exogenous L-amino acids such as L-Met or L-Leu may concentrate D-amino acids produced through BsrV, enhancing incorporation into muropeptides. In theory, this approach would make these non-canonical PG peaks easier to observe by HPLC and mass spectrometry. Given that BsrV functions to produce D-amino acids and maintain osmotolerance in all active growth stages, (Figure 2.4 & Figure 2.6), further work is warranted to analyze PG structure of exponentially growing wild-type and *bsrV* mutant cells.

Members of the *Vibrionaceae* are well known for their associations with animals, and we sought to use the symbiotic relationship between *V. fischeri* and *E. scolopes* to test for a role of BsrV in one of the bacteria-host interactions. We were unable to observe any attenuation in colonization by the mutant in either individual or competitive contexts (Figure 2.7), therefore BsrV's role in *V. fischeri* appears to lie outside of the mutualism, or at least the first 48 hours of its establishment. NCDAAs have previously been implicated in their role to regulate microbial community dynamics through D-Arg inhibition of *Caulobacter crescentus* in a synthetic community. Alvarez *et al.* found that *V. cholerae* cells lacking *bsrV* were unable to inhibit *C. crescentus* in the same way that wild-type cells could, and this effect was attributed to D-Arg (5). Future work should explore how BsrV-produced D-amino acids may benefit *V. fischeri* in microbial communities even though we find no evidence of an influence on the microbe-animal mutualism.

When competing the *bsrV* mutant against the wild type in culture, we find the wild-type strain has a competitive deficiency and the *bsrV* mutant demonstrates a 6% fitness advantage per generation. This work establishes a previously unknown fitness cost to producing BsrV and/or NCDAAs (Figure 2.8). Our bioinformatic analysis also uncovered that the BsrV homolog in *V. salmonocida* is interrupted by a transposon (Figure 2.2). This disruption of *bsrV* may eliminate a fitness disadvantage like the one we observed for *V. fischeri* in Figure 2.8. This fitness cost of *bsrV* in *V. fischeri* (Figure 2.8) could be related to the conversion of usable L-Amino acids into less directly useful D-forms, the depletion of PLP, which is a common coenzyme for many proteins, or the alteration of PG by the incorporation of NCDAAs. Competing a *V. fischeri* mutant with a largely intact but enzymatically inactive BsrV against the wild type would allow us to determine if transcription and/or translation is related to this fitness cost, or if an active enzyme is required. The co-culture experiment required cells to compete in a rich, oxygenated environment through mid-log phase growth, where resources are plentiful. Competing wild type against the *bsrV* mutant in minimally defined medium would give more clues as to which environments make BsrV most costly (or most beneficial). Further investigation into this fitness cost in other *Vibrio*'s with BsrV orthologs, such as *V. cholerae,* is also necessary to determine if this cost is unique to *V. fischeri* or if it is conserved.

Regulation may be a key factor influencing the differences between *V. fischeri* and *V. cholerae* BsrV enzymes. The absence of D-amino acid production by the wild type in minimally defined medium indicates the absence of a necessary substrate or inductor for BsrV's function. Additionally, our observations that BsrV's role extends beyond stationary phase indicates that expression of BsrV in *V. fischeri* may not be regulated through RpoS as it is in *V. cholerae.* qRT-PCR could be used to test if BsrV is, in fact, regulated by RpoS by measuring the relative

transcription of *bsrV* over time in strains that contain and lack RpoS. Finally, further exploration into the role of the large inverted repeat after the CDS of *bsrV* is necessary to determine its contribution to regulation of *bsrV* (Figure 2.2 & 2.3). The inverted repeat's regulatory role could be explored by removing the repeat from the genome of both wild-type and *bsrV* mutant strains and indirectly tested through assessing previously observed phenotypes (*e.g.* D-amino acid production and/or structural changes to PG) or directly through measuring *bsrV* mRNA via qRT-PCR.

The similarities and differences between the previously studied BsrV of *V. cholerae* and that of *V. fischeri* illuminate the importance of studying the varying biological roles of NCDAAs. Continued research elucidating novel roles for D-amino acids will shed light on many complex processes of the world that prokaryotes and eukaryotes evolved in. This study illustrates that BsrV orthologs between similar organisms can have distinct functions and provides a foundation for more comprehensive research on BsrV-produced D-amino acids.

CHAPTER 3

CONCLUSIONS AND FUTURE DIRECTIONS

The goal of this research was to gain a better understanding of the diverse roles D-amino acids serve in the context of prokaryotes. Many diverse microbial species contain BsrV orthologs that have the capability to produce abundant and diverse D-amino acids for varying biological purposes (5, 12, 13, 15). Production of these racemases and/or the roles for the D-amino acids they produce elicit a significant fitness cost, and the scope of their roles has yet to be thoroughly defined. This research expands on the current understanding of BsrV, which has primarily been explored in *V. cholerae,* by elucidating the similarities and differences between its homolog in *V. fischeri.*

Bioinformatic analysis revealed that numerous *Vibrio* species contain BsrV orthologs. Based on both phylogenetic analysis and on gene synteny, we found that *Vibrio* BsrV's fall into one of two clusters, aligning more closely with either $BsrV_{Vc}$ or $BsrV_{Vf}$. We hypothesize that the differences between these orthologs likely reflect somewhat divergent functions and may contribute to the differences we observe between BsrV's from *V. fischeri* and *V. cholerae.*

We found that as in *V. cholerae,* a *V. fischeri bsrV* mutant cannot produce wild-type levels of D-amino acids. We also found that wild-type *V. fischeri* was unable to produce D-amino acids in minimal medium that contained no L- or D-amino acids, indicating that the production of D-amino acids by BsrV is dependent on the presence of exogenous L-amino acids in the environment. Determination of the identities and abundances of such BsrV-produced NCDAAs produced by *V. fischeri*'s BsrV is an essential next step in this investigation. Amino acid chirality can be analyzed using LC-MS and HPLC using columns designed to separate

based on chirality (119). This approach will allow us to compare the specific products of BsrV from *V. fischeri* and previously reported D-amino acids produced by *V. cholerae.* I predict that the abundances of NCDAAs will be directly correlated to the corresponding exogenous L-amino acids present in the media.

The *bsrV* mutant also suffers from growth defects in low-salt environments which was similarly observed in a *V. cholerae bsrV* mutant. Collectively these observations reinforce the theory that that the production of D-amino acids contributes to the strength of the cell wall. Notably different from previous observations, is that the D-amino acid production and the low-salt growth defect was not observed in only stationary phase, but also early in mid-log growth as well. There is no reported data on NCDAA production in mid-log growth in *V. cholerae*. Therefore, a more thorough investigation into growth-dependent production of D-amino acids in *V. cholerae* is an essential next step in determining if the mid-log BsrV phenotype is unique to *V. fischeri*.

In both organisms, *bsrV* mutants have subtly altered PG structure compared to wild-type *V. fischeri*. Though we believe one of these alterations to be the incorporation of D-Met into the peptidoglycan peptide chain, there is an unidentified muropeptide that could be elucidated by further investigation. One such experiment that may shed light on these subtle PG alterations is to grow both the wild type and the *bsrV* mutant with large quantities of exogenous D-amino acids that we believe are produced, such as D-Met or D-Leu. This would allow us to see a larger percentage of muropeptides with the incorporation of specific and expected NCDAAs into the peptide chain. Additionally, it was previously demonstrated that there is a larger quantity of PG per cell in a *V. cholerae bsrV* mutant. Quantification of amount of PG per cell using ninhydrin (as described previously) (13) proved to be inconsistent in *V. fischeri.* This observation could be

explored more fully in *V. fischeri* to validate if in fact D-amino acids are governing both strength and quantity of PG during stationary phase. Additionally, investigation of muropeptides from pre-stationary phase wild-type and *bsrV* mutant cultures would clarify whether BsrV functions are unique to particular growth phases, and whether the differences seen in osmotolerance and D-AA production between *V. fischeri* and *V. cholerae* are reinforced with respect to PG alterations.

Though hopeful to find a role for BsrV within a unique symbiotic model, we found that the benefit for such a fitness cost must exist outside the *V. fischeri-E. scolopes* mutualism as our data suggests BsrV is not essential for light organ infection. Surprisingly, we found that in culture the *bsrV* mutant outcompetes the wild type. This unexpected and previously unidentified phenomenon suggests a fitness cost for D-amino acid production by BsrV which may be related to the depletion of the usable L-Amino acid pool for protein synthesis, limited free PLP, or through the process of altering PG structure.

Differences in regulation and expression of BsrV between *V. cholerae* and *V. fischeri* has not been explored. This is a necessary next step to illuminate the causes of the physiological differences we observe, such as the stationary phase versus mid-log phase D-amino acid production, of *V. cholerae* and *V. fischeri* orthologs, respectively. It is possible that *V. fischeri*'s BsrV is not regulated by RpoS, or that the large inverted repeat after the CDS of *bsrV* contributes to its expression.

It is important to study the production of D-amino acids given their presence in the environment and the distinct activities they perform in the contexts of both prokaryotes and eukaryotes. While we expanded on the current understanding of D-amino acid production by BsrV, further research is required to reveal additional unique regulatory roles they serve. For

example, investigations into the mechanisms by which D-amino acids alter PG and confer osmotolerance are essential next steps to expand this body of knowledge. Understanding the nuanced regulatory roles of D-amino acids could have promising applications in medicine and environmental research.

REFERENCES

1. Horcajo P, de Pedro MA, Cava F. 2012. Peptidoglycan plasticity in bacteria: stress-induced peptidoglycan editing by noncanonical D-amino acids. Microb Drug Resist 18:306-13.
2. Vollmer W, Blanot D, de Pedro MA. 2008. Peptidoglycan structure and architecture. FEMS Microbiol Rev 32:149-67.
3. He W, Li C, Lu CD. 2011. Regulation and characterization of the *dadRAX* locus for D-amino acid catabolism in *Pseudomonas aeruginosa* PAO1. J Bacteriol 193:2107-15.
4. He W, Li G, Yang CK, Lu CD. 2014. Functional characterization of the *dguRABC* locus for D-Glu and D-Gln utilization in *Pseudomonas aeruginosa* PAO1. Microbiology 160:2331-2340.
5. Alvarez L, Aliashkevich A, de Pedro MA, Cava F. 2018. Bacterial secretion of D-arginine controls environmental microbial biodiversity. ISME J 12:438-450.
6. Hochbaum AI, Kolodkin-Gal I, Foulston L, Kolter R, Aizenberg J, Losick R. 2011. Inhibitory effects of D-amino acids on *Staphylococcus aureus* biofilm development. J Bacteriol 193:5616-22.
7. Yu C, Li X, Zhang N, Wen D, Liu C, Li Q. 2016. Inhibition of biofilm formation by D-tyrosine: Effect of bacterial type and D-tyrosine concentration. Water Res 92:173-9.
8. Rumbo C, Vallejo JA, Cabral MP, Martinez-Guitian M, Perez A, Beceiro A, Bou G. 2016. Assessment of antivirulence activity of several D-amino acids against

Acinetobacter baumannii and *Pseudomonas aeruginosa*. J Antimicrob Chemother 71:3473-3481.

9. Kolodkin-Gal I, Romero D, Cao S, Clardy J, Kolter R, Losick R. 2010. D-amino acids trigger biofilm disassembly. Science 328:627-9.

10. Leiman SA, May JM, Lebar MD, Kahne D, Kolter R, Losick R. 2013. D-amino acids indirectly inhibit biofilm formation in *Bacillus subtilis* by interfering with protein synthesis. J Bacteriol 195:5391-5.

11. Sarkar S, Pires MM. 2015. D-Amino acids do not inhibit biofilm formation in *Staphylococcus aureus*. PLoS One 10:e0117613.

12. Aliashkevich A, Alvarez L, Cava F. 2018. New insights Into the mechanisms and biological roles of D-amino acids in complex ecosystems. Front Microbiol 9:683.

13. Lam H, Oh DC, Cava F, Takacs CN, Clardy J, de Pedro MA, Waldor MK. 2009. D-amino acids govern stationary phase cell wall remodeling in bacteria. Science 325:1552-5.

14. Cava F, de Pedro MA, Lam H, Davis BM, Waldor MK. 2011. Distinct pathways for modification of the bacterial cell wall by non-canonical D-amino acids. EMBO J 30:3442-53.

15. Espaillat A, Carrasco-Lopez C, Bernardo-Garcia N, Pietrosemoli N, Otero LH, Alvarez L, de Pedro MA, Pazos F, Davis BM, Waldor MK, Hermoso JA, Cava F. 2014. Structural basis for the broad specificity of a new family of amino-acid racemases. Acta Crystallogr D Biol Crystallogr 70:79-90.

16. Wei SL YR. 1989. Development of symbiotic bacterial bioluminescence in a nearshore cephalopod, *Euprymna scolopes*. Marine Biology 103:6.

17. Radkov AD, Moe LA. 2014. Bacterial synthesis of D-amino acids. Appl Microbiol Biotechnol 98:5363-74.

18. Hernandez SB, Cava F. 2016. Environmental roles of microbial amino acid racemases. Environ Microbiol 18:1673-85.

19. Bastings J, van Eijk HM, Olde Damink SW, Rensen SS. 2019. D-amino Acids in health and disease: A focus on cancer. Nutrients 11.

20. Yamauchi T, Choi SY, Okada H, Yohda M, Kumagai H, Esaki N, Soda K. 1992. Properties of aspartate racemase, a pyridoxal 5'-phosphate-independent amino acid racemase. J Biol Chem 267:18361-4.

21. Yoshimura T, Esak N. 2003. Amino acid racemases: functions and mechanisms. J Biosci Bioeng 96:103-9.

22. Vranova V, Zahradnickova, H., Janous, D., Skene, K.R., Matharu, A.S., Rejsek, K. and Formanek, P. 2012. The significance of D-amino acids in soil, fate and utilization by microbes and plants: review and identification of knowledge gaps. Plant and soil 354:21-39.

23. Friedman M. 1999. Chemistry, nutrition, and microbiology of D-amino acids. J Agric Food Chem 47:3457-79.

24. Azua I, Goiriena I, Bana Z, Iriberri J, Unanue M. 2014. Release and consumption of D-amino acids during growth of marine prokaryotes. Microb Ecol 67:1-12.

25. Mayer C, Kluj RM, Muhleck M, Walter A, Unsleber S, Hottmann I, Borisova M. 2019. Bacteria's different ways to recycle their own cell wall. Int J Med Microbiol 309:151326.

26. Dramsi S, Magnet S, Davison S, Arthur M. 2008. Covalent attachment of proteins to peptidoglycan. FEMS Microbiol Rev 32:307-20.

27. Neuhaus FC, Baddiley J. 2003. A continuum of anionic charge: structures and functions of D-alanyl-teichoic acids in gram-positive bacteria. Microbiol Mol Biol Rev 67:686-723.

28. Adin DM, Engle JT, Goldman WE, McFall-Ngai MJ, Stabb EV. 2009. Mutations in *ampG* and lytic transglycosylase genes affect the net release of peptidoglycan monomers from *Vibrio fischeri*. J Bacteriol 191:2012-22.

29. Quintela JC, Garcia-del Portillo F, Pittenauer E, Allmaier G, de Pedro MA. 1999. Peptidoglycan fine structure of the radiotolerant bacterium *Deinococcus radiodurans* Sark. J Bacteriol 181:334-7.

30. Quintela JC, Pittenauer E, Allmaier G, Aran V, de Pedro MA. 1995. Structure of peptidoglycan from *Thermus thermophilus* HB8. J Bacteriol 177:4947-62.

31. Caparros M, Pisabarro AG, de Pedro MA. 1992. Effect of D-amino acids on structure and synthesis of peptidoglycan in *Escherichia coli*. J Bacteriol 174:5549-59.

32. Healy VL, Lessard IA, Roper DI, Knox JR, Walsh CT. 2000. Vancomycin resistance in enterococci: reprogramming of the D-ala-D-Ala ligases in bacterial peptidoglycan biosynthesis. Chem Biol 7:R109-19.

33. Bruckner H, Westhauser T. 2003. Chromatographic determination of L- and D-amino acids in plants. Amino Acids 24:43-55.

34. Kubota T, Kobayashi T, Nunoura T, Maruyama F, Deguchi S. 2016. Enantioselective utilization of D-amino acids by deep-sea microorganisms. Front Microbiol 7:511.

35. Radkov AD, McNeill K, Uda K, Moe LA. 2016. D-Amino acid catabolism is common among soil-dwelling bacteria. Microbes Environ 31:165-8.

36. Bruckner H, Schieber A. 2001. Ascertainment of D-amino acids in germ-free, gnotobiotic and normal laboratory rats. Biomed Chromatogr 15:257-62.

37. Franklin FC, Venables WA. 1976. Biochemical, genetic, and regulatory studies of alanine catabolism in *Escherichia coli* K12. Mol Gen Genet 149:229-37.

38. Lobocka M, Hennig J, Wild J, Klopotowski T. 1994. Organization and expression of the *Escherichia coli* K-12 *dad* operon encoding the smaller subunit of D-amino acid dehydrogenase and the catabolic alanine racemase. J Bacteriol 176:1500-10.

39. Marshall VP, Sokatch JR. 1968. Oxidation of D-amino acids by a particulate enzyme from *Pseudomonas aeruginosa*. J Bacteriol 95:1419-24.

40. Pollegioni L, Piubelli L, Sacchi S, Pilone MS, Molla G. 2007. Physiological functions of D-amino acid oxidases: from yeast to humans. Cell Mol Life Sci 64:1373-94.

41. Raunio RP, Straus LD, Jenkins WT. 1973. D-alanine oxidase from *Escherichia coli*: participation in the oxidation of L-alanine. J Bacteriol 115:567-73.

42. Tanigawa M, Shinohara T, Saito M, Nishimura K, Hasegawa Y, Wakabayashi S, Ishizuka M, Nagata Y. 2010. D-Amino acid dehydrogenase from *Helicobacter pylori* NCTC 11637. Amino Acids 38:247-55.

43. Xu J, Bai Y, Fan T, Zheng X, Cai Y. 2017. Expression, purification, and characterization of a membrane-bound D-amino acid dehydrogenase from *Proteus mirabilis* JN458. Biotechnol Lett 39:1559-1566.

44. Jones RM, Jr., Popham DL, Schmidt AL, Neidle EL, Stabb EV. 2018. *Vibrio fischeri* DarR Directs Responses to D-Aspartate and Represents a Group of Similar LysR-Type Transcriptional Regulators. J Bacteriol 200.

45. Fleming A. 1929. On the antibacterial action of cultures of a penicillium, with special reference to their use in the isolation of *B. influenzae*. British Journal of Experimental Pathology 10:226-236.

46. Sieber SA, Marahiel MA. 2005. Molecular mechanisms underlying nonribosomal peptide synthesis: approaches to new antibiotics. Chem Rev 105:715-38.

47. Kano S, Suzuki S, Hara R, Kino K. 2019. Synthesis of D-amino acid-containing dipeptides using the adenylation domains of nonribosomal peptide synthetase. Appl Environ Microbiol 85.

48. Nishanth Kumar S, Dileep C, Mohandas C, Nambisan B, Ca J. 2014. Cyclo(D-Tyr-D-Phe): a new antibacterial, anticancer, and antioxidant cyclic dipeptide from *Bacillus* sp. N strain associated with a rhabditid entomopathogenic nematode. J Pept Sci 20:173-85.

49. Sasabe J, Suzuki M. 2019. Distinctive roles of D-amino acids in the homochiral world: Chirality of amino acids modulates mammalian physiology and pathology. Keio J Med 68:1-16.

50. Balu DT, Takagi S, Puhl MD, Benneyworth MA, Coyle JT. 2014. D-Serine and serine racemase are localized to neurons in the adult mouse and human forebrain. Cell Mol Neurobiol 34:419-35.

51. Ito T, Hayashida M, Kobayashi S, Muto N, Hayashi A, Yoshimura T, Mori H. 2016. Serine racemase is involved in D-Aspartate biosynthesis. J Biochem 160:345-353.

52. Fossat P, Turpin FR, Sacchi S, Dulong J, Shi T, Rivet JM, Sweedler JV, Pollegioni L, Millan MJ, Oliet SH, Mothet JP. 2012. Glial D-Serine gates NMDA receptors at excitatory synapses in prefrontal cortex. Cereb Cortex 22:595-606.

53. D'Ascenzo M, Podda MV, Grassi C. 2014. The role of D-serine as co-agonist of NMDA receptors in the nucleus accumbens: relevance to cocaine addiction. Front Synaptic Neurosci 6:16.

54. Potier B, Turpin FR, Sinet PM, Rouaud E, Mothet JP, Videau C, Epelbaum J, Dutar P, Billard JM. 2010. Contribution of the D-Serine-dependent pathway to the cellular mechanisms underlying cognitive aging. Front Aging Neurosci 2:1.

55. Sasabe J, Miyoshi Y, Suzuki M, Mita M, Konno R, Matsuoka M, Hamase K, Aiso S. 2012. D-amino acid oxidase controls motoneuron degeneration through D-serine. Proc Natl Acad Sci U S A 109:627-32.

56. Wu SZ, Bodles AM, Porter MM, Griffin WS, Basile AS, Barger SW. 2004. Induction of serine racemase expression and D-serine release from microglia by amyloid beta-peptide. J Neuroinflammation 1:2.

57. Ota N, Shi T, Sweedler JV. 2012. D-Aspartate acts as a signaling molecule in nervous and neuroendocrine systems. Amino Acids 43:1873-86.

58. D'Aniello S, Somorjai I, Garcia-Fernandez J, Topo E, D'Aniello A. 2011. D-Aspartic acid is a novel endogenous neurotransmitter. FASEB J 25:1014-27.

59. Lozupone CA, Stombaugh JI, Gordon JI, Jansson JK, Knight R. 2012. Diversity, stability and resilience of the human gut microbiota. Nature 489:220-30.

60. Sasabe J, Miyoshi Y, Rakoff-Nahoum S, Zhang T, Mita M, Davis BM, Hamase K, Waldor MK. 2016. Interplay between microbial D-amino acids and host D-amino acid oxidase modifies murine mucosal defence and gut microbiota. Nat Microbiol 1:16125.

61. Rosini E, Pollegioni L, Ghisla S, Orru R, Molla G. 2009. Optimization of D-amino acid oxidase for low substrate concentrations--towards a cancer enzyme therapy. FEBS J 276:4921-32.

62. Sasabe J, Suzuki M. 2018. Emerging role of D-amino acid metabolism in the innate defense. Front Microbiol 9:933.

63. Connolly JP, Goldstone RJ, Burgess K, Cogdell RJ, Beatson SA, Vollmer W, Smith DG, Roe AJ. 2015. The host metabolite D-serine contributes to bacterial niche specificity through gene selection. ISME J 9:1052.

64. Coburn B, Sekirov I, Finlay BB. 2007. Type III secretion systems and disease. Clin Microbiol Rev 20:535-49.

65. Navarro Llorens JM, Tormo A, Martinez-Garcia E. 2010. Stationary phase in gram-negative bacteria. FEMS Microbiol Rev 34:476-95.

66. Grossman AD. 1995. Genetic networks controlling the initiation of sporulation and the development of genetic competence in *Bacillus subtilis*. Annu Rev Genet 29:477-508.

67. Hu H, Emerson J, Aronson AI. 2007. Factors involved in the germination and inactivation of *Bacillus anthracis* spores in murine primary macrophages. FEMS Microbiol Lett 272:245-50.

68. McKevitt MT, Bryant KM, Shakir SM, Larabee JL, Blanke SR, Lovchik J, Lyons CR, Ballard JD. 2007. Effects of endogenous D-alanine synthesis and autoinhibition of *Bacillus anthracis* germination on *in vitro* and *in vivo* infections. Infect Immun 75:5726-34.

69. Bartlett TM, Bratton BP, Duvshani A, Miguel A, Sheng Y, Martin NR, Nguyen JP, Persat A, Desmarais SM, VanNieuwenhze MS, Huang KC, Zhu J, Shaevitz JW, Gitai Z. 2017. A periplasmic polymer curves *Vibrio cholerae* and promotes pathogenesis. Cell 168:172-185 e15.

70. Holtje JV. 1998. Growth of the stress-bearing and shape-maintaining murein sacculus of *Escherichia coli*. Microbiol Mol Biol Rev 62:181-203.

71. Hengge-Aronis R. 2002. Recent insights into the general stress response regulatory network in *Escherichia coli*. J Mol Microbiol Biotechnol 4:341-6.

72. Doublet P, van Heijenoort J, Mengin-Lecreulx D. 1992. Identification of the *Escherichia coli murI* gene, which is required for the biosynthesis of D-glutamic acid, a specific component of bacterial peptidoglycan. J Bacteriol 174:5772-9.

73. Kato S, Hemmi H, Yoshimura T. 2012. Lysine racemase from a lactic acid bacterium, *Oenococcus oeni*: structural basis of substrate specificity. J Biochem 152:505-8.

74. Kuan Y-C, et al. 2011. Biochemical characterization of a novel lysine racemase from *Proteus mirabilis* BCRC10725. Process Biochemistry 46:1914-1920.

75. Matsui D, Oikawa T, Arakawa N, Osumi S, Lausberg F, Stabler N, Freudl R, Eggeling L. 2009. A periplasmic, pyridoxal-5'-phosphate-dependent amino acid racemase in *Pseudomonas taetrolens*. Appl Microbiol Biotechnol 83:1045-54.

76. Radkov AD, Moe LA. 2018. A broad spectrum racemase in *Pseudomonas putida* KT2440 plays a key role in amino acid catabolism. Front Microbiol 9:1343.

77. McFall-Ngai MJ, Ruby EG. 1991. Symbiont recognition and subsequent morphogenesis as early events in an animal-bacterial mutualism. Science 254:1491-4.

78. Stabb EV. 2006. The *Vibrio fischeri-Euprymna scolopes* light organ symbiosis. ASM Press, Washington D.C.

79. Boettcher KJ, Ruby EG. 1990. Depressed light emission by symbiotic *Vibrio fischeri* of the sepiolid squid *Euprymna scolopes*. J Bacteriol 172:3701-6.

80. Boettcher KJ RE, McFallNgai MJ. 1996. Bioluminescence in the symbiotic squid *Euprymna scolopes* is controlled by a daily biological rhythm. Journal of Comparative Physiology A 179:9.

81. Ruby EG, Urbanowski M, Campbell J, Dunn A, Faini M, Gunsalus R, Lostroh P, Lupp C, McCann J, Millikan D, Schaefer A, Stabb E, Stevens A, Visick K, Whistler C, Greenberg EP. 2005. Complete genome sequence of *Vibrio fischeri*: a symbiotic bacterium with pathogenic congeners. Proc Natl Acad Sci U S A 102:3004-9.

82. Stabb EV, Ruby EG. 2002. RP4-based plasmids for conjugation between *Escherichia coli* and members of the *Vibrionaceae*. Methods Enzymol 358:413-26.

83. Dunn AK, Millikan DS, Adin DM, Bose JL, Stabb EV. 2006. New *rfp*- and pES213-derived tools for analyzing symbiotic *Vibrio fischeri* reveal patterns of infection and *lux* expression *in situ*. Appl Environ Microbiol 72:802-10.

84. Ruby EG. 1999. The *Euprymna scolopes*-*Vibrio fischeri* symbiosis: a biomedical model for the study of bacterial colonization of animal tissue. J Mol Microbiol Biotechnol 1:13-21.

85. Aschtgen MS, Lynch JB, Koch E, Schwartzman J, McFall-Ngai M, Ruby E. 2016. Rotation of *Vibrio fischeri* flagella produces outer membrane v esicles that induce host development. J Bacteriol 198:2156-65.

86. Montgomery MK, McFall-Ngai M. 1994. Bacterial symbionts induce host organ morphogenesis during early postembryonic development of the squid *Euprymna scolopes*. Development 120:1719-29.

87. Troll JV, Adin DM, Wier AM, Paquette N, Silverman N, Goldman WE, Stadermann FJ, Stabb EV, McFall-Ngai MJ. 2009. Peptidoglycan induces loss of a nuclear peptidoglycan recognition protein during host tissue development in a beneficial animal-bacterial symbiosis. Cell Microbiol 11:1114-27.

88. Sycuro LK, Ruby EG, McFall-Ngai M. 2006. Confocal microscopy of the light organ crypts in juvenile *Euprymna scolopes* reveals their morphological complexity and dynamic function in symbiosis. J Morphol 267:555-68.

89. Nyholm SV, Stabb EV, Ruby EG, McFall-Ngai MJ. 2000. Establishment of an animal-bacterial association: recruiting symbiotic *Vibrios* from the environment. Proc Natl Acad Sci U S A 97:10231-5.

90. Jones BW NM. 2004. Counterillumination in the Hawaiian Bobtail squid, *Euprymna scolopes*. Marine Biology 144:5.

91. DeLoney-Marino CR, Wolfe AJ, Visick KL. 2003. Chemoattraction of *Vibrio fischeri* to serine, nucleosides, and *N*-acetylneuraminic acid, a component of squid light-organ mucus. Appl Environ Microbiol 69:7527-30.

92. Nyholm SV, McFall-Ngai MJ. 2003. Dominance of *Vibrio fischeri* in secreted mucus outside the light organ of *Euprymna scolopes*: the first site of symbiont specificity. Appl Environ Microbiol 69:3932-7.

93. Montgomery MK, McFall-Ngai M. 1993. Embryonic development of the light organ of the sepiolid squid *Euprymna scolopes* Biol Bull 184:296-308.

94. Ruby EG, Asato LM. 1993. Growth and flagellation of *Vibrio fischeri* during initiation of the sepiolid squid light organ symbiosis. Arch Microbiol 159:160-7.

95. Koropatnick TA, Engle JT, Apicella MA, Stabb EV, Goldman WE, McFall-Ngai MJ. 2004. Microbial factor-mediated development in a host-bacterial mutualism. Science 306:1186-8.

96. Foster JS, McFall-Ngai MJ. 1998. Induction of apoptosis by cooperative bacteria in the morphogenesis of host epithelial tissues. Dev Genes Evol 208:295-303.

97. Doino JA, McFall-Ngai MJ. 1995. A transient exposure to symbiosis-competent bacteria induces light organ morphogenesis in the host squid. Biol Bull 189:347-355.

98. Nyholm SV, McFall-Ngai MJ. 1998. Sampling the light-organ microenvironment of *Euprymna scolopes*: description of a population of host cells in association with the bacterial symbiont *Vibrio fischeri*. Biol Bull 195:89-97.

99. Lee KH, Ruby EG. 1994. Effect of the squid host on the abundance and distribution of symbiotic *Vibrio fischeri* in nature. Appl Environ Microbiol 60:1565-71.

100. Typas A, Banzhaf M, Gross CA, Vollmer W. 2011. From the regulation of peptidoglycan synthesis to bacterial growth and morphology. Nat Rev Microbiol 10:123-36.

101. Dunn AK, Martin MO, Stabb EV. 2005. Characterization of pES213, a small mobilizable plasmid from *Vibrio fischeri*. Plasmid 54:114-34.

102. Hanahan D. 1983. Studies on transformation of *Escherichia coli* with plasmids. J Mol Biol 166:557-80.

103. Bertani G. 1951. Studies on lysogenesis. I. The mode of phage liberation by lysogenic Escherichia coli. J Bacteriol 62:293-300.

104. Stabb EV, Reich KA, Ruby EG. 2001. *Vibrio fischeri* genes *hvnA* and *hvnB* encode secreted NAD(+)-glycohydrolases. J Bacteriol 183:309-17.

105. Septer AN, Wang Y, Ruby EG, Stabb EV, Dunn AK. 2011. The haem-uptake gene cluster in *Vibrio fischeri* is regulated by Fur and contributes to symbiotic colonization. Environ Microbiol 13:2855-64.

106. McCann J, Stabb EV, Millikan DS, Ruby EG. 2003. Population dynamics of *Vibrio fischeri* during infection of *Euprymna scolopes*. Appl Environ Microbiol 69:5928-34.

107. Altschul SF, Gish W, Miller W, Myers EW, Lipman DJ. 1990. Basic local alignment search tool. J Mol Biol 215:403-10.

108. Kanehisa M, Goto S. 2000. KEGG: Kyoto encyclopedia of genes and genomes. Nucleic Acids Res 28:27-30.

109. Kingsford CL, Ayanbule K, Salzberg SL. 2007. Rapid, accurate, computational discovery of Rho-independent transcription terminators illuminates their relationship to DNA uptake. Genome Biol 8:R22.

110. Mrazek J, Xie S. 2006. Pattern locator: a new tool for finding local sequence patterns in genomic DNA sequences. Bioinformatics 22:3099-100.

111. Almagro Armenteros JJ, Tsirigos KD, Sonderby CK, Petersen TN, Winther O, Brunak S, von Heijne G, Nielsen H. 2019. SignalP 5.0 improves signal peptide predictions using deep neural networks. Nat Biotechnol 37:420-423.

112. Oberto J. 2013. SyntTax: a web server linking synteny to prokaryotic taxonomy. BMC Bioinformatics 14:4.

113. Hayashi K. 1975. A rapid determination of sodium dodecyl sulfate with methylene blue. Analytical Biochemistry 67:503-6.

114. Popham DL, Helin J, Costello CE, Setlow P. 1996. Analysis of the peptidoglycan structure of *Bacillus subtilis* endospores. J Bacteriol 178:6451-8.

115. Boyd A, Krikos A, Simon M. 1981. Sensory transducers of *E. coli* are encoded by homologous genes. Cell 26:333-43.

116. Scheurwater E, Reid CW, Clarke AJ. 2008. Lytic transglycosylases: bacterial space-making autolysins. Int J Biochem Cell Biol 40:586-91.

117. Lee KH, Ruby EG. 1994. Competition between *Vibrio fischeri* strains during initiation and maintenance of a light organ symbiosis. J Bacteriol 176:1985-91.

118. Stabb EV, Ruby EG. 2003. Contribution of *pilA* to competitive colonization of the squid *Euprymna scolopes* by *Vibrio fischeri*. Appl Environ Microbiol 69:820-6.

119. Ilisz I, Berkecz R, Peter A. 2008. Application of chiral derivatizing agents in the high-performance liquid chromatographic separation of amino acid enantiomers: a review. J Pharm Biomed Anal 47:1-15.